Construction and Characterization of a Torsional Pendulum that Detects a Novel Form of Cranial Energy

John Norman Hansen* and Joshua A. Lieberman

Department of Chemistry and Biochemistry, University of Maryland

College Park, MD 20742

*Corresponding Author

Author Contact:

J. Norman Hansen
Department of Chemistry and Biochemistry
University of Maryland
College Park, MD 20742
Email: nhansen@umd.edu

Running Title: *Chi Pendulum*

Title

Construction and Characterization of a Torsional Pendulum that Detects a Novel Form of Cranial Energy

Authors and Affiliations

John Norman Hansen*
Department of Chemistry and Biochemistry
University of Maryland
College Park, MD 20742
nhansen@umd.edu
*Corresponding Author

Joshua A. Lieberman
Department of Chemistry and Biochemistry
University of Maryland
College Park, MD 20742
joshua.lieberman@gmail.com

Abstract

A torsional pendulum consisting of a dome-shaped energy collector and a nylon monofilament support fiber was suspended above the cranium of a seated human subject and the effects of the subject on the oscillations of the pendulum were measured. There were dramatic effects, with FFT analysis of the oscillation signal showing many new frequencies in addition to the natural frequency of 0.034 *Hz*. The lowest new frequencies (0.0-0.002 *Hz*) were accompanied by a shift in the Center of Oscillation (*COO*) of the pendulum, and the higher frequencies were associated with changes in the amplitude of oscillation. The ΔCOO (7.3 *deg*) and the amplitude (12 *deg*) effects were substantial, and would require forces equivalent to 34 and 56 *mg*, respectively. Residual effects on the ΔCOO and amplitudes persisted for at least 30 *min* after the subject departed, and the rate at which they subsided conformed to the kinetics of a chemical relaxation process with a relaxation time (τ) of 600 *sec*. Shifts in the magnitude of the ΔCOO with the subject present also conformed to chemical relaxations processes, with τ values of 35 and 200 *sec*. It is proposed that the energy that drives the anomalous oscillations when the subject is present is the result of enzyme-mediated energy transductions that convert metabolic energy into a form of energy that can affect the pendulum. Although highly speculative, it is suggested that aspects of quantum entanglement are involved in the energy transduction process.

Introduction

The idea that living organisms are surrounded by fields of bio-energy is widespread, and is the basis of many forms of traditional medicine that have been practiced for thousands of years. The existence of bio-energy fields is questioned because experimental scientists have been unable to detect them. Since the ability to detect, measure, and quantify is required for the scientific study of anything, our inability to detect them precludes their study. However, the fact that these fields have not been detected does not prove they do not exist. It is possible that the means that have been chosen to detect them have not been suitable, whereas an alternate means might detect them easily.

In this paper, we describe a detector that responds to an energy field with novel properties in the vicinity of the cranium of a human subject The detector consists of a simple torsional pendulum suspended by a short length of nylon monofilament. Torsional pendulums are notable for their ability to perform highly sensitive measurements, despite their simplicity. The oscillatory motions of the pendulum are observed using a real-time video object-tracking program. We call this device a *Chi* Pendulum, with *Chi* being the Greek letter *X*, and the form of energy it detects, we call *Chi* energy. This name is inspired by the Chinese word for bio-energy, *qi*, usually pronounced "chee."

The results we have obtained with this Pendulum are astonishing. They point to a form of energy whose qualities, to our knowledge, have heretofore not been observed. For example, there is a component of the force that acts like a spinning vortex that can vary in direction and intensity. The magnitude of the force is significant and easily measured and characterized by the movements of the Pendulum. Other aspects of this force will be described as they are encountered during the presentation of the *Results*, and in the *Discussion*.

Results

The physical characteristics of the Pendulum used in these experiments

A drawing of the Pendulum is in *Figure 1*, and its components are shown in *Figure 2*. The assembly and operation of the Pendulum are described in *Materials and Methods*. Briefly, it is a dome-shaped energy collector constructed of steel mesh that looks like window screen. It is suspended from an adjustable-height support by a short length of nylon monofilament. The Pendulum is set in motion by a puff of air and its oscillatory behavior is observed using real-time video object tracking. If the Pendulum behaves as a damped simple harmonic oscillator (*sho*), it should conform to the equation for a torsional-spring damped *sho*,

Equation 1: $y = \mathrm{A}(e^{-\gamma t})cos(\omega t)$,

where y is the displacement at any time, A is the displacement at $t = 0$, ω is the frequency of oscillation in *radians/sec*, and γ in sec^{-1} is the coefficient of damping which is mainly due to air resistance. Although a complete *sho* equation includes a phase term, *Equation 1* is a simplified version that assumes a phase of zero in which A_{max} is at $t = 0$. This equation is available in standard physics texts and on-line sources (search terms: torsional spring, torsional pendulum, damped harmonic oscillator).

Figure 3 shows the oscillation of the Pendulum. It is highly damped, and the amplitude of the oscillation diminishes rapidly toward the Center of Oscillation (*COO*). Using the principles of signal analysis, the frequency components of the oscillation signal can be analyzed, as described in *Materials and Methods*. Using the SigView program which implements the Fast Fourier Transform (FFT) version of the Fourier Transform, the frequencies were analyzed, with *Figure 4* showing the FFT result. A single peak with a frequency of 0.034 *Hz* was obtained, which corresponds to a period of 29.4 *sec*.

Figure 1

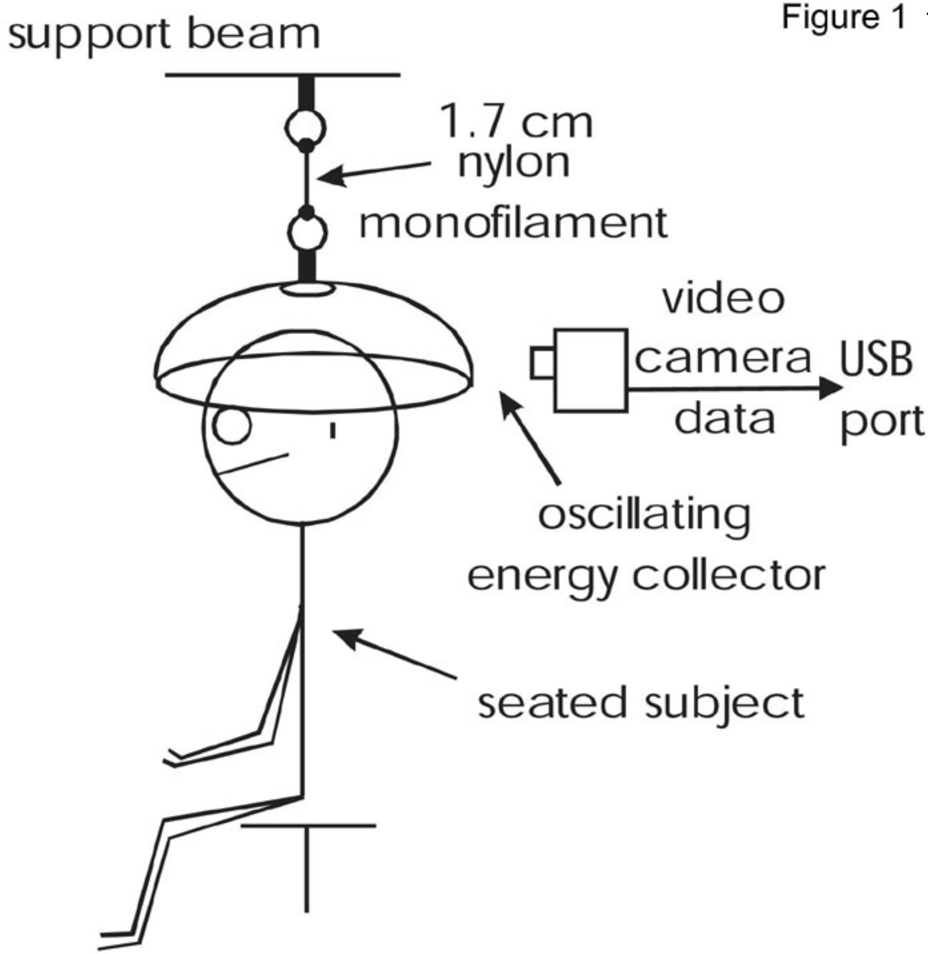

Figure 1. **Subject seated under Pendulum with video object-tracking camera.** Pendulum components are shown in *Figure 2* and described in *Materials and Methods*.

Figure 2 .

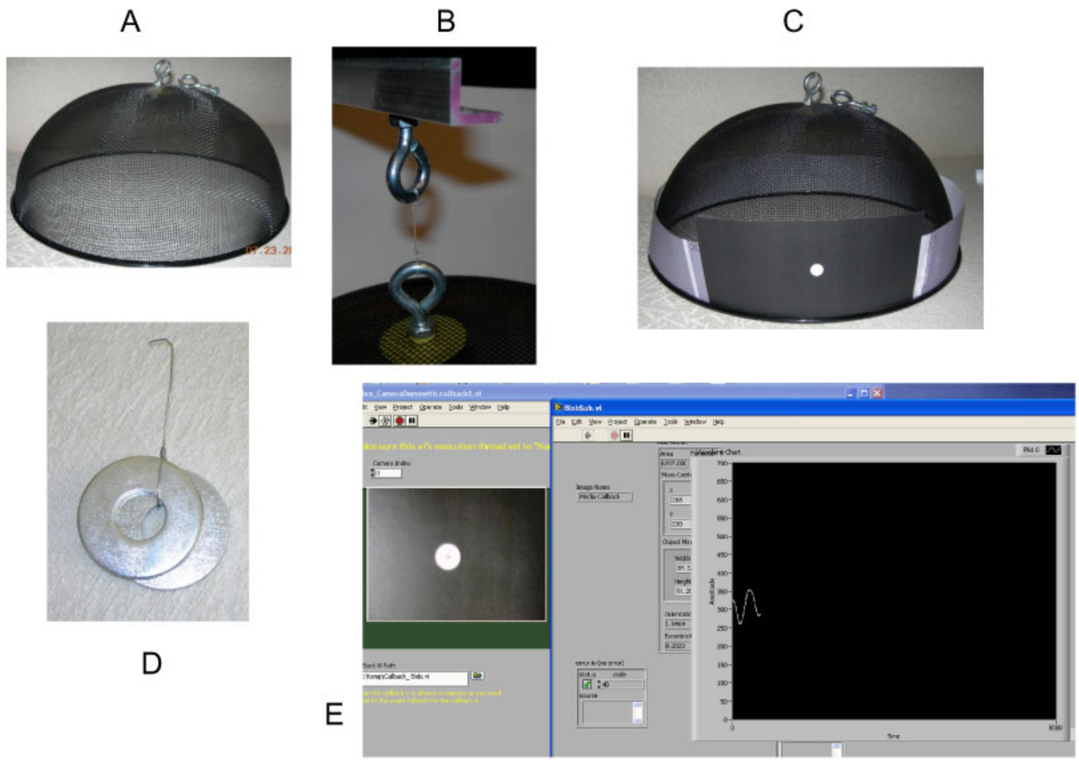

Figure 2. **Components of the Pendulum and data collection.** Also see *Materials and Methods*. A. Dome-shaped collector with eye-bolts. B. Attachment of collector to aluminum angle-beam using two 2.5 *cm* diameter eye-bolts and a 1.7 *cm* nylon monofilament connecting between them. C. Target for Object Tracking. A 1-*cm* white dot on a black background, printed onto standard white copy paper using a laser printer. D. Steel washers (4.5 *cm* diameter, ~27 *g*) used to add weight to the outer rim of the Pendulum to alter its frequency of oscillation for measurements of the torsional constant (κ) as described in *Materials and Methods* and *Figure 5*. E. A screenshot of the computer display during data collection. It displays the position of the 1 *cm* white dot superimposed by a small red circle showing the calculated center of the white dot, the continuously-updated dimensions of the white dot, and a graphical record of the position of the center of the white dot as the experiment progresses.

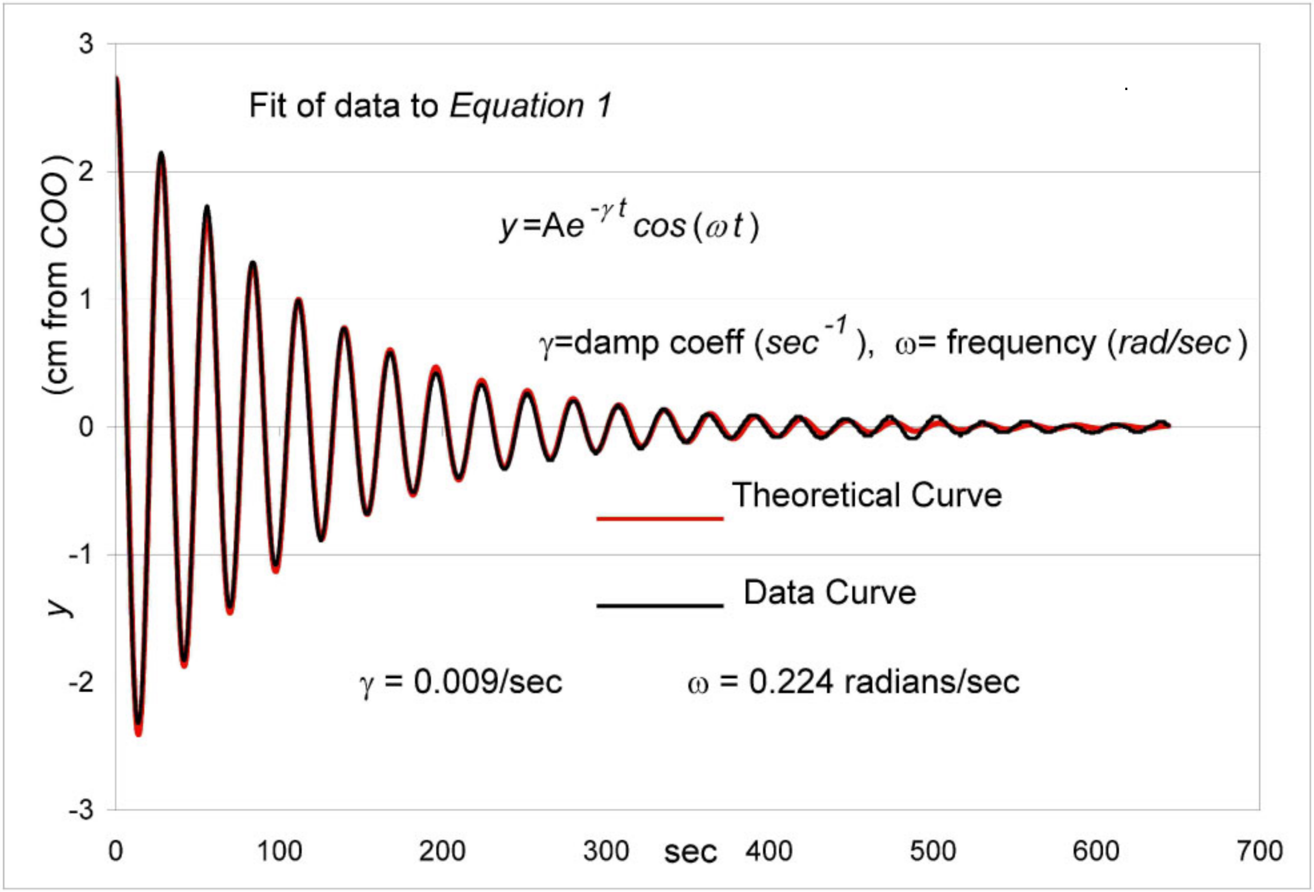

Figure 3. **The Pendulum behaves as a damped simple harmonic oscillator (*sho*).** The *black* curve represents the data point measurements of the deflection of the Pendulum from the *Center of Oscillation* (*COO*) taken at a rate of 10/*sec*. The *red* curve is the theoretical curve predicted by *Equation 1* (see *Results*) in which the values of ω (*frequency*) and γ (*damping coefficient*) are chosen to give a best fit to the data. The best-fit ω is 0.224 *radians/sec*, and the best-fit γ is 0.009/*sec*.

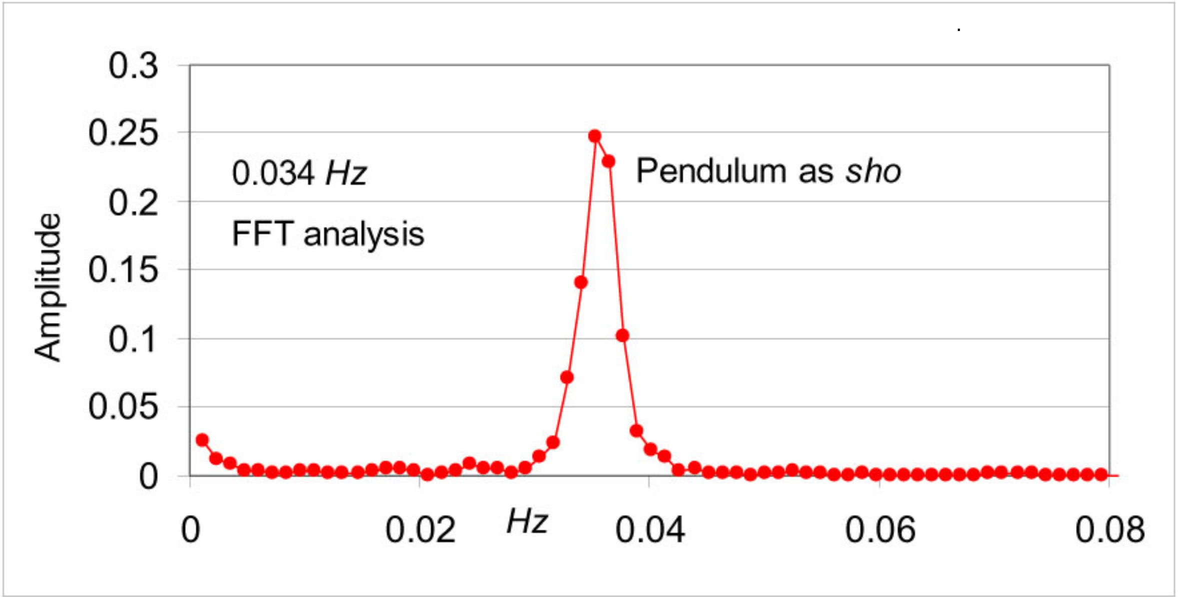

Figure 4. **FFT of natural oscillations of the Pendulum**. FFT analysis of the data in *Figure 3* using SigView as described in *Materials and Methods*. It shows that the natural frequency of the Pendulum, in the absence of a Subject, is about 0.034 *Hz*, which is equivalent to a period of 29.4 *sec*.

Equation 1 was used to calculate a theoretical curve with ω and γ chosen to give a best fit to the experimental data. *Figure 3* shows the theoretical curve superimposed on the data curve, in which the theoretical curve had a ω of 0.22 *radians/sec*, and a γ of 0.00900/*sec*. The fit of the data curve to the theoretical curve is excellent, including the region in which damping has been extensive. This shows both that the Pendulum behaves as a nearly-ideal damped *sho*, and that the ambient conditions surrounding the Pendulum have negligible effects on its behavior. Other than assuring that no sources of moving air (heating, cooling, fans, etc.) were present, no additional measures to isolate the Pendulum from environmental conditions were necessary to attain this excellent performance. Although temperature gradients that would generate moderate air turbulence were surely present in the environment, one can conclude that the Pendulum was insensitive to them. We conclude that even small deviations of the Pendulum from ideal behavior in the presence of a Subject are significant and represent effects exerted by the Subject.

In order to use the Pendulum as a tool to measure the magnitudes of the forces being exerted on it, the data in *Figure 5* were used to estimate the torsional constant (κ) of the nylon monofilament support, which in turn can be used to determine the force that is required to rotationally-displace the Pendulum a particular distance from its *COO*. The equation that describes the force-displacement relationship is:

Equation 2 $\omega^2 = \kappa/I$,

where ω is the oscillatory frequency (*radians/sec*), κ is the torsional constant (*dyne-cm/radian*) of the nylon fiber, and I (*g-cm*^{2}) is the *Moment of Inertia* of the Pendulum, in which the mass is assumed to be concentrated in a ring located at an experimentally-determined radius. *Figure 5* and *Materials and Methods* describe the estimation of κ, which was determined to be 2,240 *dyne-cm/radian*, or 39 *dyne-cm/deg* of rotation. As described in *Materials and Methods*, the force required to displace the Pendulum by 1 *deg* of rotation is equal to the force exerted by a 4.6 *mg* mass resting on a horizontal surface at 1 *G*. A conversion factor of 4.6 *mg/deg* of rotation of the Pendulum is used in experiments described below.

Behavior of the Pendulum in the presence of a Subject

This Pendulum has been under study for several years, and hundreds of experiments have been performed. The results presented here show phenomena that have appeared consistently throughout these experiments, differing only in the quality of the data as a consequence of refinements of the Pendulum and the method of data collection. The current Pendulum, which is optimized with respect to natural frequency, together with the use of real-time video object tracking, has eliminated ambiguities that had previously detracted from the quality of the results. *Figure 6* shows the effect that the presence of a Subject has on the oscillations of the Pendulum. In this experiment, the Subject sat under the Pendulum when it was undergoing small oscillations around its natural *COO*, remained there for about 15 *min*, and then departed (*Seg 1*). The Pendulum was allowed to damp out for several *min*, whereupon the Subject sat under it again for about 25 *min*, and departed (*Seg 2*). After an additional several *min* of damping, the Subject returned for another 18 *min*, and departed (*Seg 3*). The Pendulum was then allowed to damp out

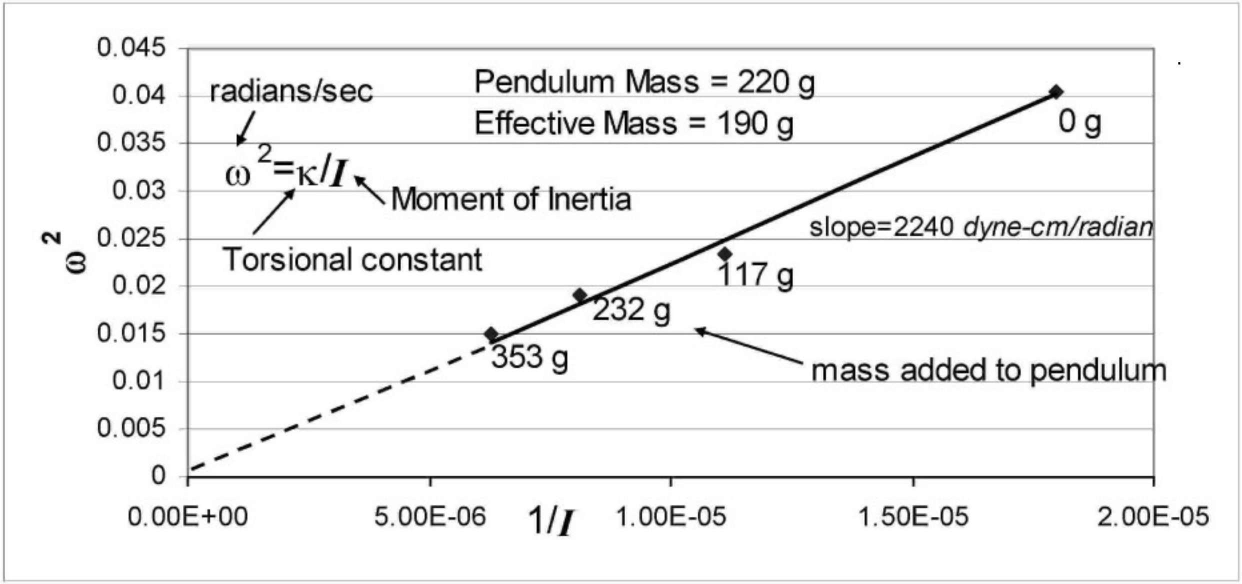

Figure 5. **Determination of torsional constant (κ) of the nylon filament of the Pendulum**. This is described in *Results* and *Materials and Methods*. The *Figure* shows the effect of adding masses to the outer rim of the Pendulum on the ω of the Pendulum. The data are fitted to *Equation 2* (*Results*), which gives a κ of 2,240 *dyne-cm/radian*, or 39 *dyne-cm/deg* of rotation. A conversion factor of 4.6 *mg/deg* of rotation is obtained.

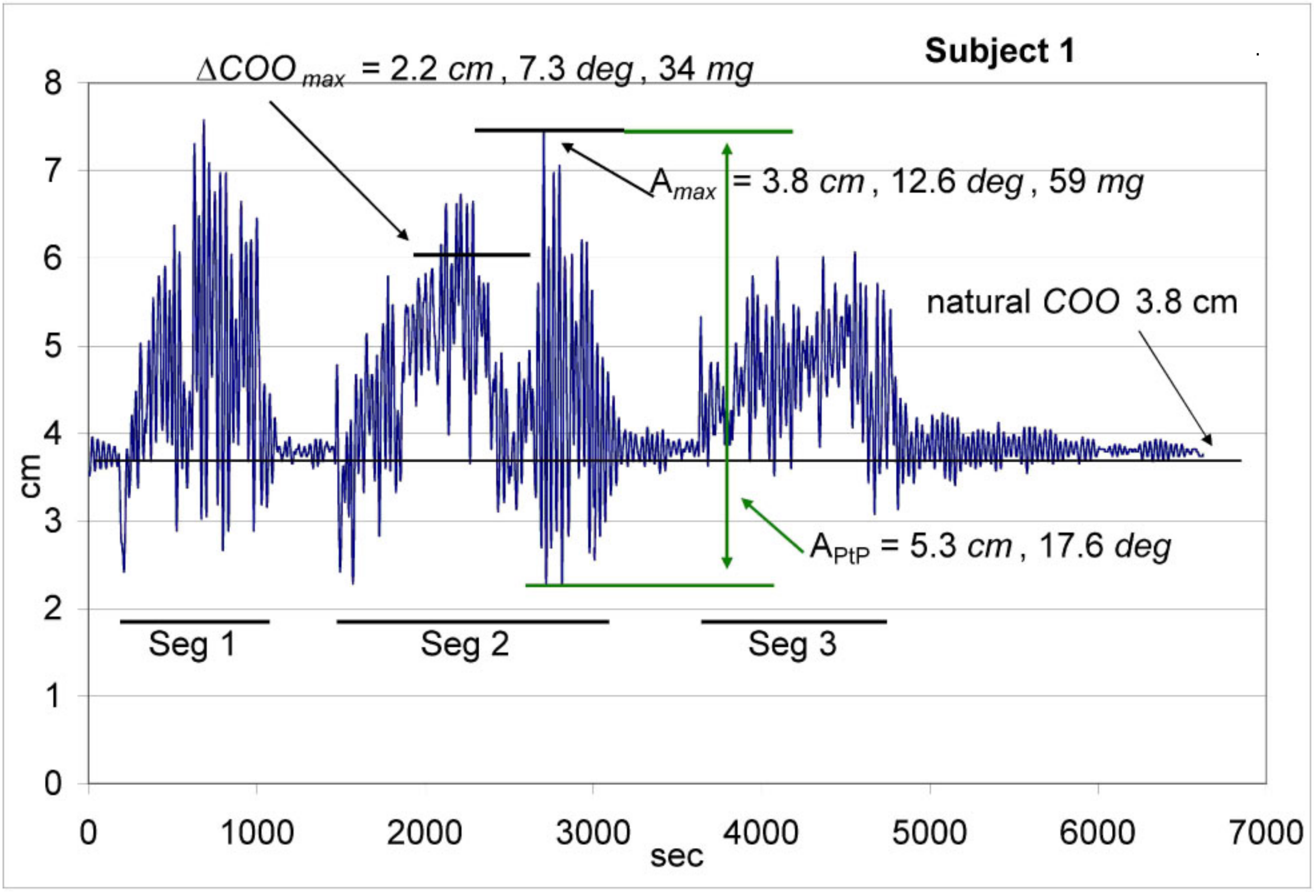

Figure 6. **Patterns of oscillation of Pendulum when Subject 1 is present.** The initial seconds of the experiment are oscillations prior to Subject 1 being seated under the Pendulum. The *cm* scale represents movements of the Pendulum in which positive values represent movements in the *clockwise direction* as viewed *looking downward* from *above* the Pendulum. *Seg 1* is a period of time during which Subject 1 is seated under the Pendulum, as are *Seg 2* and *Seg 3*, respectively. When the Subject is present, the amplitudes of the oscillations and the Center of Oscillation (*COO*) of the Pendulum both change dramatically, with the maximum ΔCOO being indicated for *Seg 2*, expressed as *cm*, *deg* of rotation, and *mg* of force required to drive the rotation. A_{max} is the maximum amplitude of the displacement from the natural *COO* expressed as *cm*, *deg* of rotation, and *mg* of force. The vertical *green* arrow is the A_{PtP}, which is the largest peak-to-peak amplitude observed during the experiment, expressed as *cm* and *deg* of rotation. When the Subject departs the Pendulum after each *Seg*, the Pendulum reverts toward the natural *COO*, but it does not actually attain classical *sho* behavior until long after the Subject departs, as described in *Results* and in *Figures 14-18*.

toward its natural *COO* for an additional 30 *min* (*post-Seg 3*). During the *post Seg 3* period of damping, all persons left the room for another part of the building. Although the Subject did not come in contact with the Pendulum at any time during any of the *Seg*s, the effects on the Pendulum were dramatic. These effects included the induction of large amplitude swings that oscillated around a *COO* that was dramatically shifted away from the natural *COO*.

Focus on Seg 2 data

Whereas *Figure 6* provides a global view of what occurred during this multi-*Seg* experiment, it is useful to focus on a single *Seg*, to better interpret what is happening. *Figure 7* focuses on *Seg 2*, from about 1400 to 3500 *sec*. As would be expected from the behavior of the Pendulum in the absence of a Subject (*Figure 3*), the Pendulum consistently returns toward the natural *COO* whenever the Subject is not seated under the Pendulum. However, when the Subject is seated under the Pendulum, it displays a dramatically-altered behavior. In each *Seg*, as soon as the Subject is seated, the Pendulum begins to oscillate with a dramatically-increased amplitude. In addition to increased amplitudes of oscillation, in all 3 *Segs* of the experiment, the *COO* of the Pendulum slowly shifts away from the natural *COO*. The shift of the *COO* is largest in *Seg 2*, although the shifts in *Segs 1* and *3* are nearly as large. Accordingly, in *Seg 2*, the ΔCOO_{max} is 2.2 *cm*, which corresponds to 7.3 *deg*, which is equivalent to a force exerted by a mass of 33.6 *mg* pressing on a horizontal surface at 1 *G*. Moreover, for a time period of 10 *min*, the ΔCOO is so large that there is only one swing of the Pendulum that even crosses the natural *COO*. The fact that the natural *COO* has not changed at any time is demonstrated by the fact that the Pendulum returns toward the natural *COO* whenever the Subject departs.

This extended-time displacement of the *COO* is extraordinary, and constitutes one of the most important aspects of the energy that is being detected by the Pendulum. Whereas it is conceivable that the increased amplitudes when the Subject is under the Pendulum are due to air currents created by the Subject, it is highly unlikely that random air currents could exert the kind of spirally-directed force that would be necessary to rotationally-deflect the *COO* of the Pendulum for such extended periods of time. The ability of random air currents to do this is refuted by control experiments presented at the end of this *Results* section.

Analysis of the frequency components of the Seg 2 oscillation profile

Figure 8 shows the FFT analysis of the time period when the Subject was under the Pendulum in *Seg 2*. The highest frequency amplitude is about 0.032 *Hz*, which corresponds to the natural frequency in the absence of a Subject (*Figure 4*). However, in contrast to *Figure 4*, which shows only the natural frequency, the FFT in the presence of the Subject shows many new frequencies. The BandPass and BandStop filters in SigView (*Materials and Methods*) were used to analyze how these frequencies contributed to the behavior of the Pendulum. Starting with the lowest frequencies, *Figure 9* shows the 0.0-0.002 *Hz* BandPass component overlaid on the unfiltered signal of *Seg 2*. This analysis shows that the 0.0-0.002 *Hz* frequency range correlates with displacements of the Pendulum from its natural *COO*. Close examination of the

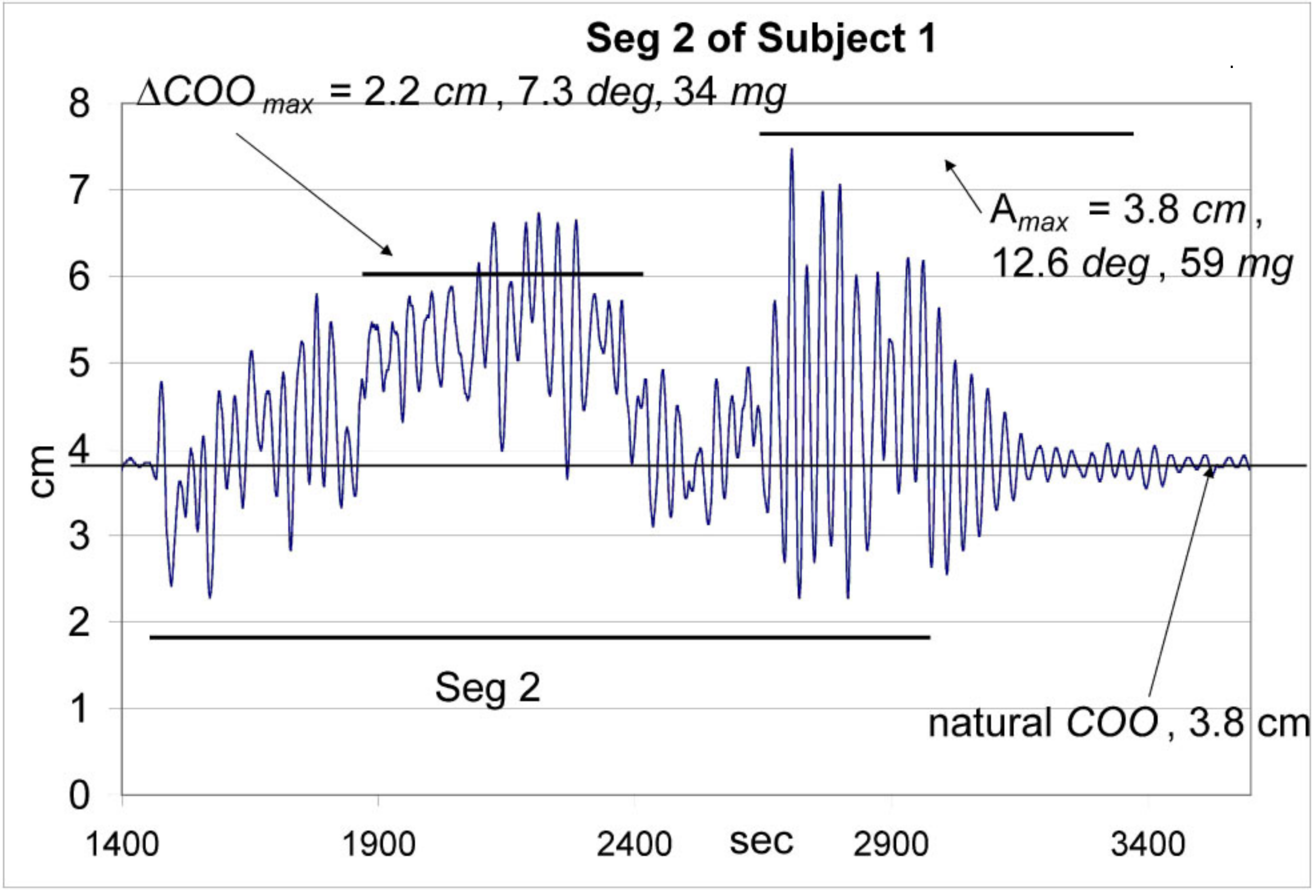

Figure 7. **Focus on *Seg 2* of *Figure 6* data**. *Figure 6* shows the results of three consecutive experiments with *Subject 1* under the Pendulum. *Figure 7* focuses on *Seg 2* data of *Figure 6*. The duration of *Seg 2* is about 1,700 *sec* (28 *min*), and during that time, the *COO* shifts 2.2 *cm* away from the natural *COO*. This corresponds to 7.3 *deg* of rotation, and based on the **κ** of the monofilament fiber, would require a force that is equivalent to 34 *mg*.

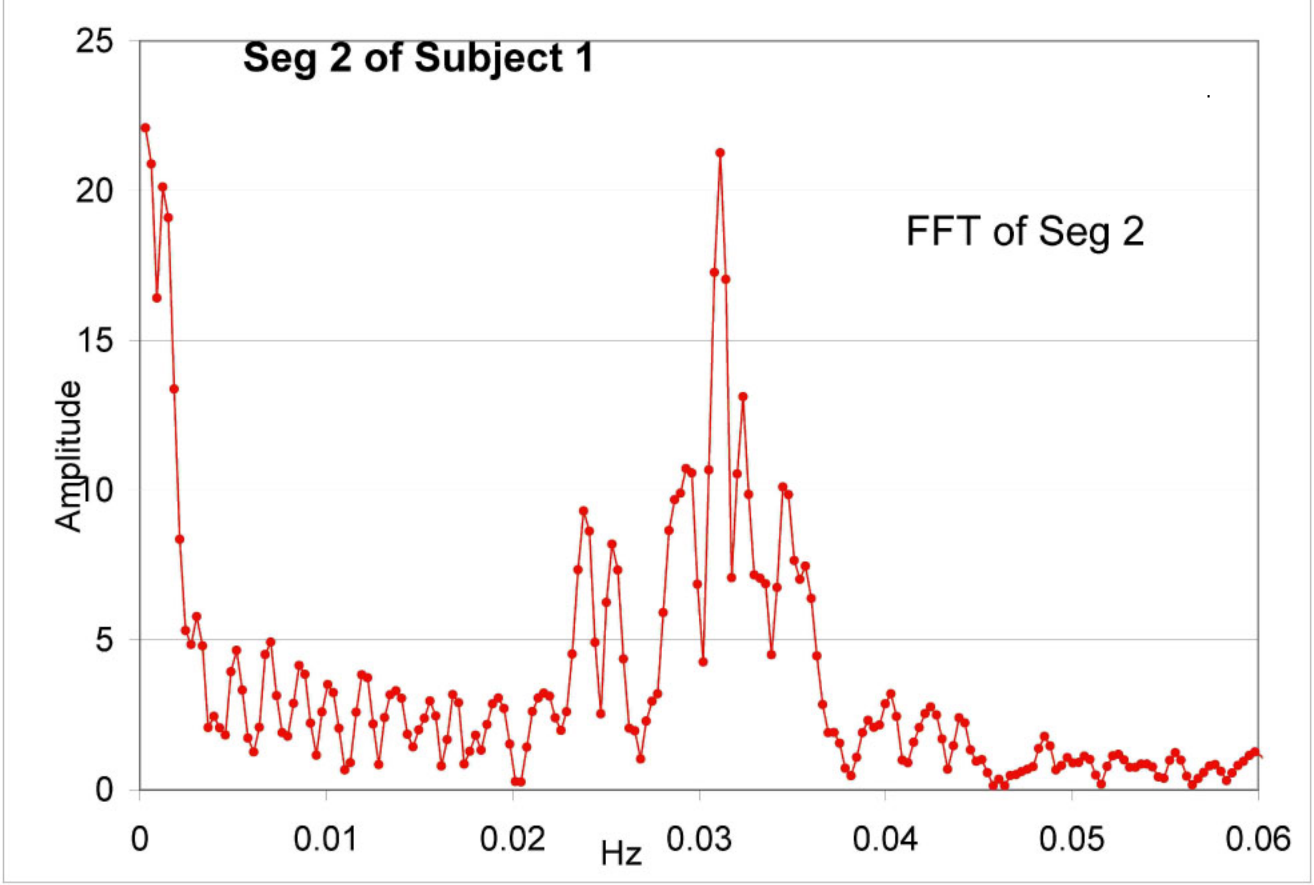

Figure 8. **FFT analysis of the *Seg 2* data of *Figure 7*.** SigView (*Materials and Methods*) was used to analyze the frequency components that contribute to the oscillation data in *Figure 7*. The major frequency peak is at 0.032 *Hz*, but there are other frequencies that are also significant. These significant frequencies encompass the entire range of 0.0-0.06 *Hz* (higher frequencies are small and are not shown). The frequencies that contribute to the *Sig 2* profile are further analyzed in *Figure 10*.

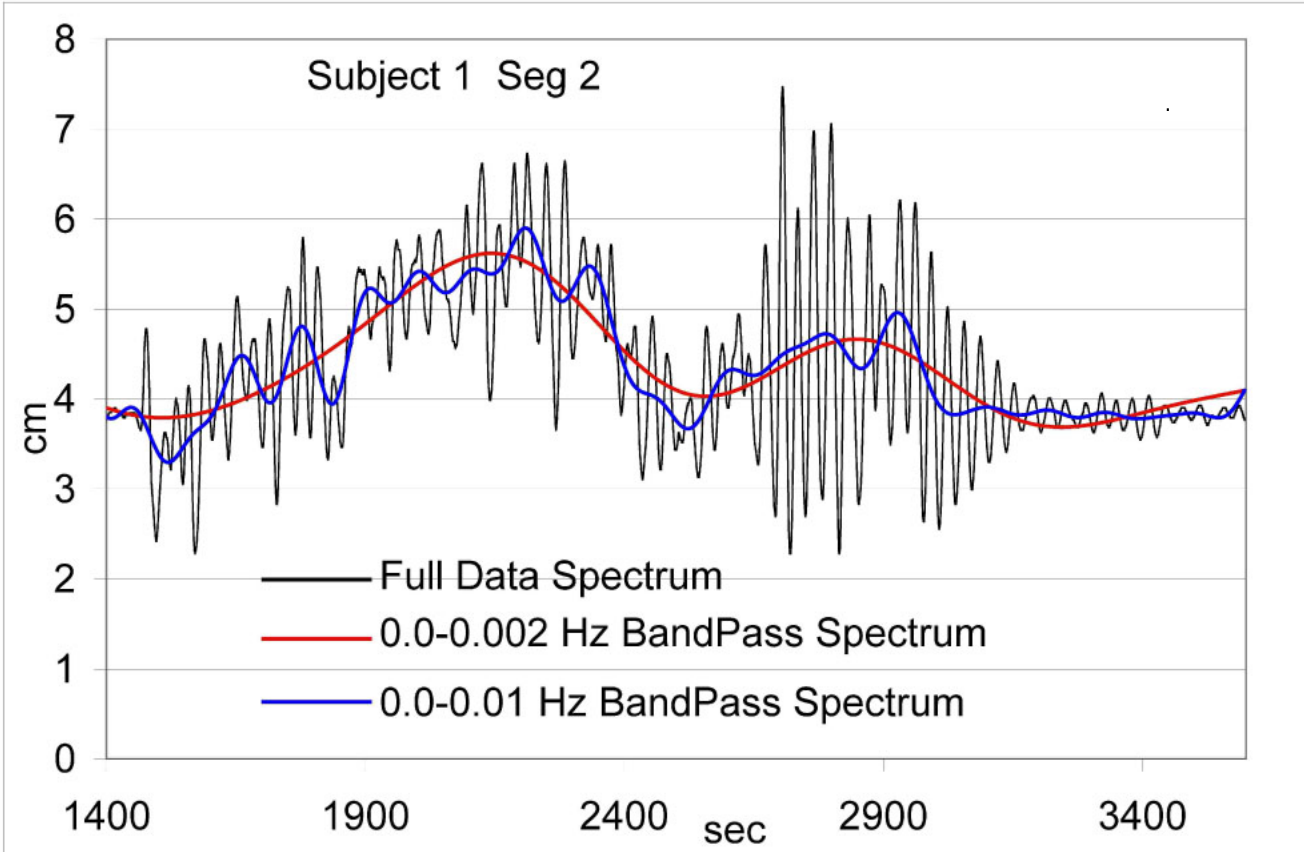

Figure 9. **Low-frequency BandPass overlays onto the Pendulum oscillation profile.** The *Seg 2* data profile of *Figure 7* is shown as overlaid with 0.0-0.02 *Hz* (*red curve*) and 0.0-0.01 *Hz* (*blue curve*) BandPass (BP) profiles. The 0.0-0.02 BP follows the general pattern of *COO* displacements. The 0.0-0.01 BP closely tracks the mid-points of all the oscillation swings throughout the profile, including the time-period after the Subject leaves the Pendulum (see *Results*).

oscillation profile shows that each swing of the Pendulum has a mid-point, and these mid-points shift from swing-to-swing. Whereas the 0.0-0.02 Hz BandPass profile follows the shifts in these mid-points in a general way, an overlay of the 0.0-0.01 Hz BandPass profile shows that this expanded frequency range tracks these mid-points very closely. This separates the effect on the *COO* from the effect on amplitudes of oscillation. It is the lower frequencies (0.0-0.01 *Hz*) that are related to the deflections of the *COO* away from the natural *COO*, whereas the higher frequencies are related to the enhancement of the amplitudes of oscillation.

This approach was used to analyze the other major components of the frequency spectrum in *Figure 8*, with the results in *Figure 10*. The *right top panel* of *Figure 10* shows the unfiltered oscillation signal from *Seg 2* of Subject 1 as shown in *Figure 7*. The *A-G profiles* below that represent the BandPass frequency components that contribute to the *top panel* profile, and correspond to the frequency peaks in the FFT analysis in the *left panel*. The *A profile* of *Figure 10* accordingly shows the contribution of the "0.034-0.038 Hz" frequency range to the *top panel* profile. The *B profile* shows the contribution of the "0.032-0.034 Hz" contribution to the *top panel* profile. The *C-G profiles* show the contributions of other frequencies, respectively. The *A-E profiles* show frequencies that are relatively strong, whereas the *F-G profiles* show frequencies that are relatively weak. Frequencies that are weaker than *F-G* are not shown.

As we try to extract meaning from these profiles, we consider that the Pendulum has a particular natural frequency at which it oscillates in the absence of a Subject, which in *Figure 4*, was about 0.034 *Hz*. It is reasonable to expect that in the presence of a Subject, this natural frequency would be a major component frequency. The highest peak (*E*) in the FFT profile in *Figure 10* is about 0.032 *Hz*, although there is a smaller peak (*B*) at 0.034 *Hz*, both of which are near the natural frequency. Since these correspond to the natural frequency, they would be expected to persist throughout the entire experiment, but the results belie this expectation. For example, the *E* frequency component does not become strong until the last half of the *Seg* which follows the period of time during which the ΔCOO is large. The *B* frequency undulates throughout, but becomes near-zero amplitude during the time that the ΔCOO is at a maximum. Indeed, through much of the time during which the ΔCOO is large, neither the *B* nor the *E* component makes a major contribution. Examination of the other frequency components show that during the time of large ΔCOO displacement, it is the *A* frequency and the *C* frequency that become stronger. Neither *A* nor *C* is close to the natural frequency; instead, they are above and below the natural frequency, respectively, with each flanking the *B* peak in a symmetrical fashion. This is echoed by the *D* frequency, which has near zero amplitude when ΔCOO is large, and becomes significant only when the ΔCOO is small, during the last half of the *Seg*. On the whole, a striking aspect of this analysis is that there is no frequency that persists throughout the entire *Seg*, but each rises and falls in a unique pattern. One consistent feature is that when the amplitude of any one of the frequencies goes through a maximum, there is another that goes through a minimum, so that peaks in one profile generally align with troughs in one or more other profiles. Someone looking at these data without having any knowledge of the construction of the Pendulum, might conclude that the *Moment of Inertia* was undergoing periodic changes in magnitude, but that would violate Newton's laws. Exploring the significance of these patterns will require many additional experiments, which are beyond the scope of this paper.

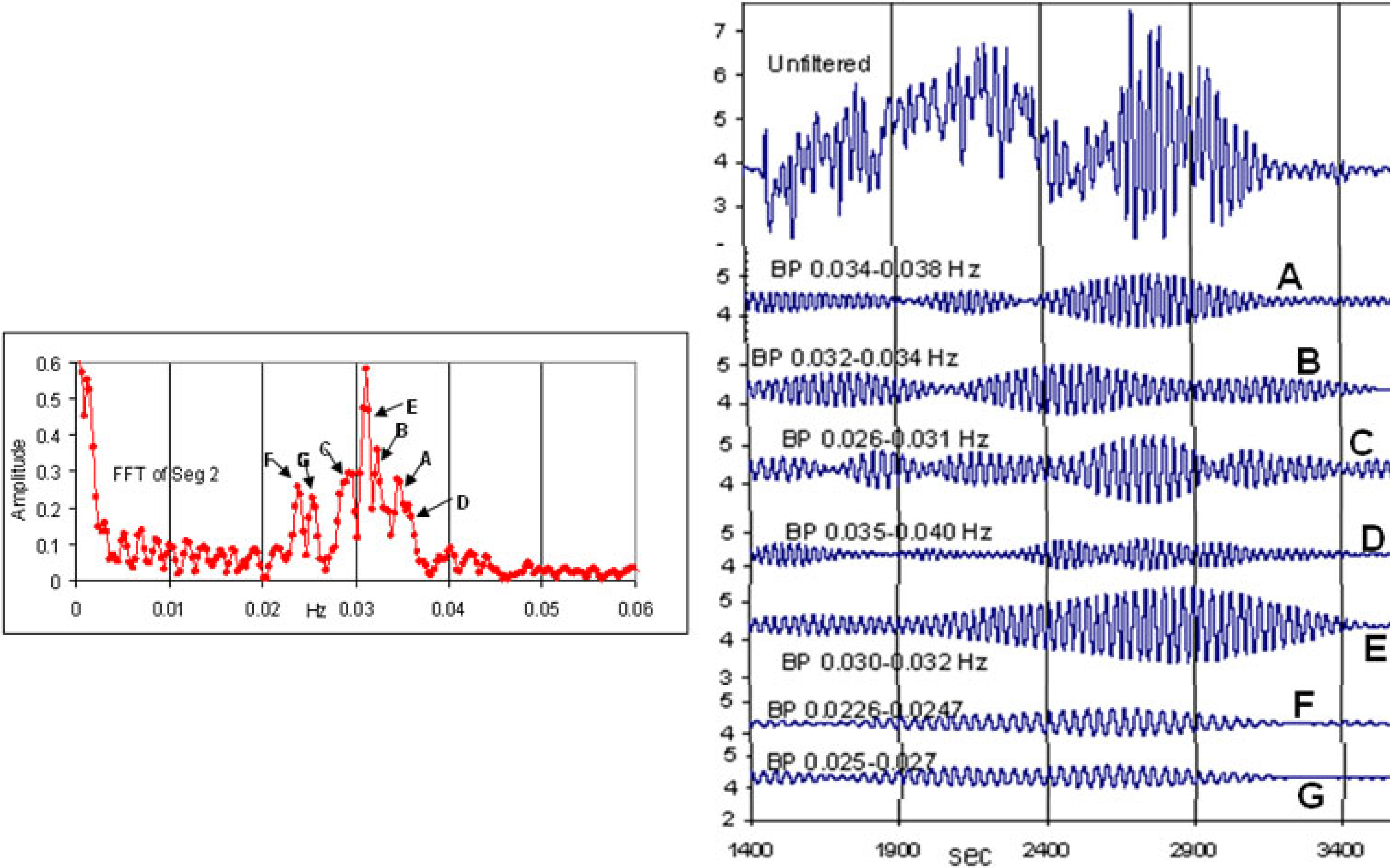

Figure 10. **Frequency components that contribute to the oscillation profile of *Seg 2*.** The *right top panel* shows oscillation data of *Seg 2*, including several *min* after the Subject left the Pendulum. The FFT analysis of these data is shown in the *left panel*. Each of the *A-G* frequency peaks corresponds to a particular frequency range that is responsible for that peak. The contribution of each peak is assessed by applying a BandPass filter to the frequency range that is defined by the lowest amplitudes above and below each peak. For curves *A-G*, what is represented is the BandPass (BP) profile that represents the frequency contribution of that particular BP component to the *top panel* data, *e.g.*, *curve A* is what is obtained by applying a 0.034-0.038 Hz BandPass filter to the top panel data.

The effects of the Subject on the patterns of oscillation are variable

The *Seg 2* profile reveals oscillation patterns that undergo variation in the other *Segs*. *Figure 11* shows the FFT analyses of *Segs 1, 2, 3* aligned so that they can be compared. An aspect that is constant among the three FFT profiles is that there are many higher and lower frequencies that surround the fundamental frequency of the Pendulum. Whereas all three *Segs* show the 0.0-0.002 *Hz* component that correlates with the "spinning vortex" effect, there is much variation among the higher frequencies, up to the 0.06 *Hz* that is displayed (magnitudes of higher frequencies were small, so are not shown).

Characterization of the Pendulum oscillations when the COO is highly displaced

Since this Pendulum is an *sho*, it should accelerate as it moves from its maximum displacement toward its *COO*, and as it crosses the *COO*, its velocity should be at a maximum and its acceleration zero. During *Seg 2* of the experiment in *Figure 7*, the ΔCOO_{max} is 2.2 *cm* away from the natural *COO*. It is reasonable to question whether the oscillations around this displaced *COO* obey the same rules as for the natural *COO*. That is to ask, when the Pendulum crosses the displaced *COO*, will it be moving at the highest velocity that is achieved during that oscillation? If it is, then one can argue that the *COO* is truly displaced, *i.e.,* the displaced *COO* has replaced the natural *COO* as the *COO* around which the Pendulum is oscillating. Because the position of the Pendulum was sampled at a rate of 10*/sec*, the velocity at any time is readily calculated. *Figure 12* shows the velocities of the Pendulum during the period of time in *Seg 2* during which the *COO* is most highly displaced. These velocities are plotted below the corresponding Pendulum displacements. The maximum velocities correlate very well with the mid-points of their respective oscillations, which argues that the displaced oscillations are "obeying the rules" of an *sho*, which in turn argues that the "displaced oscillations" are, in fact, displaced, and that the Pendulum is oscillating around the displaced *COO* instead of the natural *COO*. This argues that the motions of the Pendulum are not just a consequence of being jolted around by random forces, but that there is a spiral force that acts in such a sustained fashion that the Pendulum can be dramatically displaced from its natural *COO* for extended periods of time, and that while this displacement occurs, the Pendulum behaves as an *sho* that is oscillating around this displaced *COO*.

Anomalous Pendulum oscillations after the Subject departs

Figure 3 established that in the absence of a Subject, the Pendulum behaves as a nearly-ideal damped *sho*. Whereas a classical *sho* can be altered from its natural oscillation by an outside driving force, whenever such a force stops, it should immediately return to its natural pattern of oscillation. *Figure 13* shows that the Pendulum conforms to this expectation, in that it immediately reverts to its natural pattern of oscillation after being subjected to intermittent puffs of air. Accordingly, the *COO* displacements and amplitude modulations exerted by the Subject should abate immediately upon the Subject's departure from the Pendulum, and the Pendulum should immediately return to its ideal behavior. To a first approximation, this indeed occurs--as reflected by the fact that when the Subject departs after each *Seg* (*Figure 6*), the Pendulum proceeds toward the natural *COO*, accompanied by a damping process. However, a close examination of

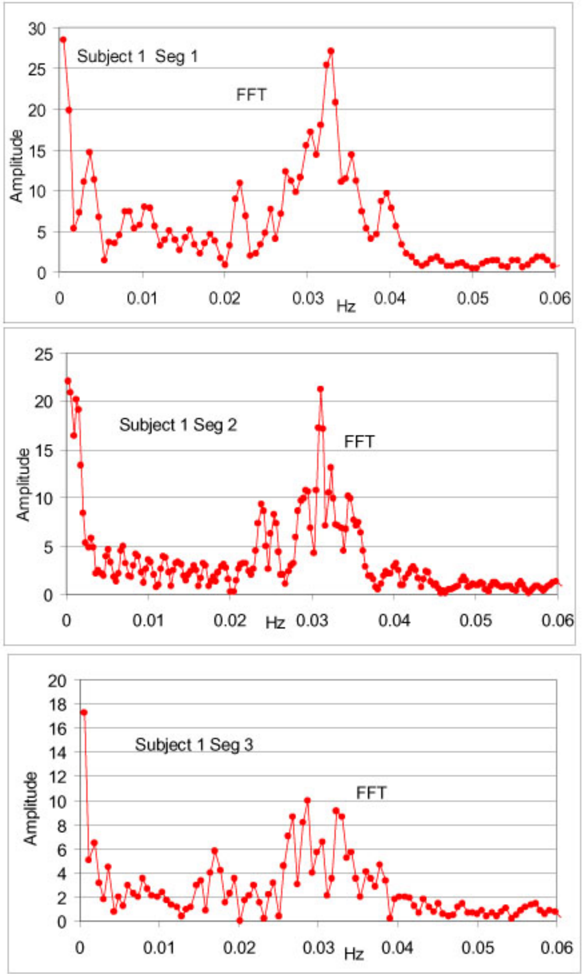

Figure 11. **FFT analysis of *Segs 1-3* of the Subject 1 data shown in *Figure 6*.** The FFT profiles are aligned vertically so that differences between them can be compared. A complete analysis of the contributions of the frequency peaks in the *Seg 2* FFT profile is shown in *Figure 10*.

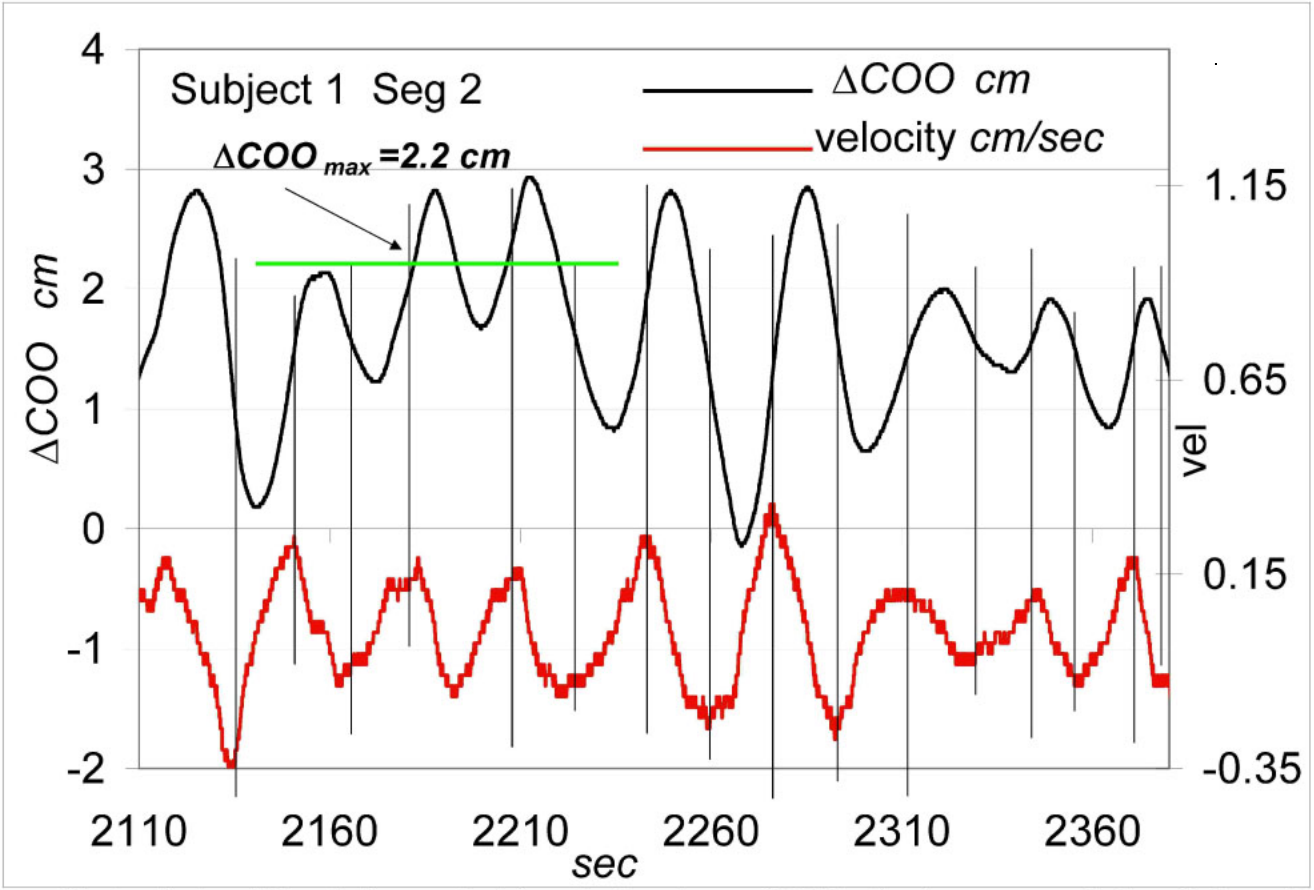

Figure 12. Analysis of Pendulum velocities during large ΔCOO displacements of *Seg 2* data from *Figure 7*. The *top curve (black)* shows the oscillations of the Pendulum during the most highly-displaced region of *Seg 2* of *Figure 7*. The *bottom curve (red)* shows the velocities (positive and negative) of the Pendulum during these oscillations. A vertical line is drawn through each velocity maximum to establish the time during each oscillation that the Pendulum is moving most rapidly. This point corresponds to the mid-point of each swing. The significance of this is described in the *Results*.

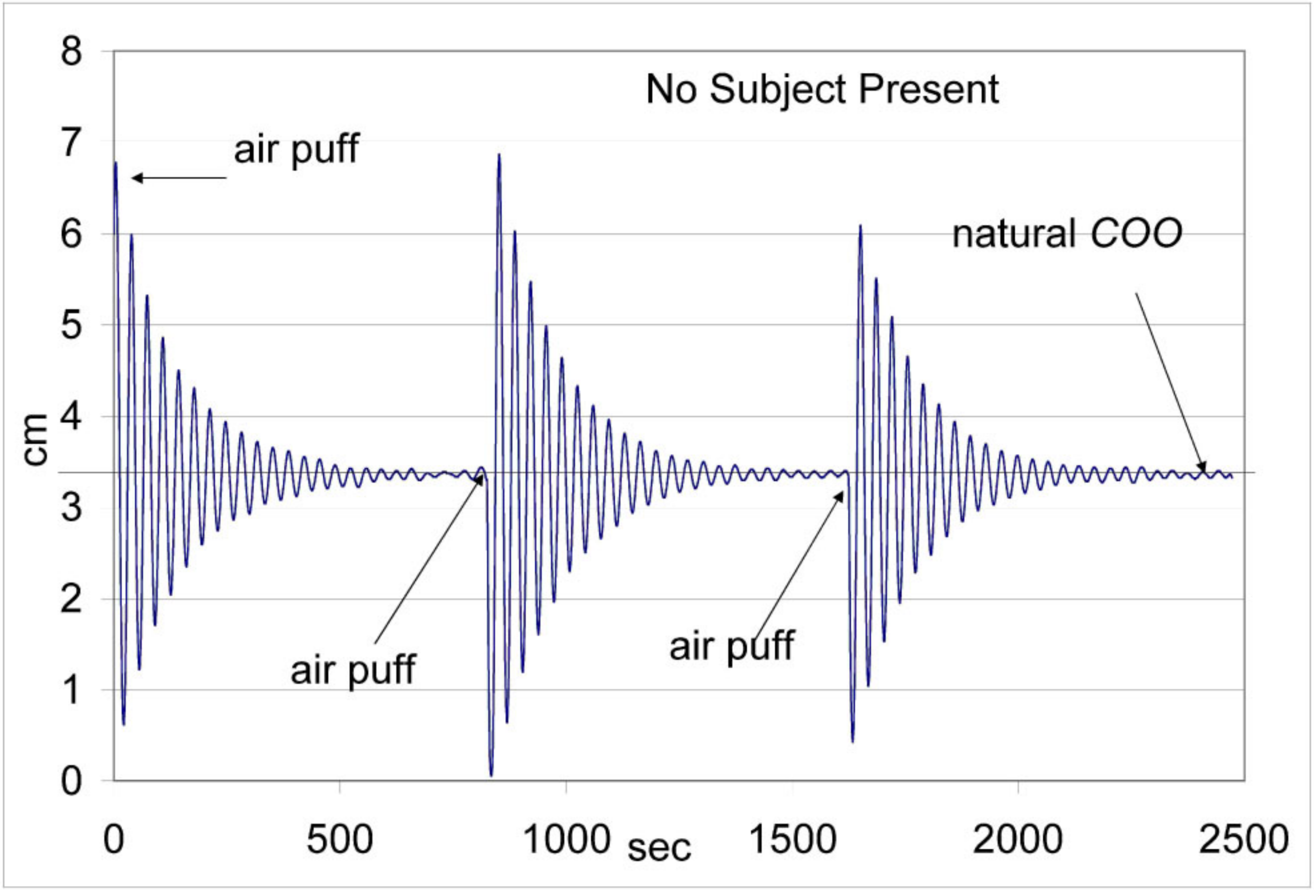

Figure 13. **Oscillation of the Pendulum when no Subject is present.** This is similar to *Figure 3*, except that the Pendulum oscillations are induced by successive puffs of air (see *Materials and Methods*), each of which is followed by a period of damping toward the natural *COO*. As described in *Results*, after each air puff, the Pendulum immediately reverts to classical damped *sho* behavior, with no residual effects being discernable. This is in contrast to after the Subject departs the Pendulum after *Seg 3* (*Figure 14*), in which substantial residual effects exerted by the Subject persist for at least 30 *min*.

what occurs after the Subject departs after *Seg 3* belies this simple expectation. Instead of immediately resuming the classical behavior of a damped *sho*, it retains significant residual characteristics of the oscillatory patterns of when the Subject was under the Pendulum. These residual characteristics are manifested in a variety of ways that suggest retention of the vibrational frequencies that had been evident while the Subject was present during *Seg 3*.

Figure 14 shows the time period immediately after the end of *Seg 3*, *i.e.,* after the Subject has departed (*post Seg 3*). It is evident that the reversion to classical *sho* behavior did not occur, as shown by superimposing a theoretical damping profile (using ω and γ values from *Figure 3*) onto *Figure 14*. The kinetics of damping in the theoretical and experimental profiles are quite different, with the theoretical curve being damped much more rapidly than the experimental curve. Moreover, the oscillation envelope of the experimental curve is highly irregular, indicating that the oscillations represent multiple frequencies, which is confirmed by the FFT analysis in *Figure 15*. There is a large peak at 0.033 *Hz* which corresponds to the natural frequency of the Pendulum. To better reveal the other frequencies, the FFT was subjected to a 0.03-0.035 *Hz* BandStop to remove this peak, with the result in *Figure 16*. Many peaks are evident, appearing greater in number than when the Subject was present, suggesting that the oscillations become chaotic after the Subject departs. Included among these frequencies are the lowest-frequency components that are associated with displacement from the natural *COO*, as shown by superimposing the 0.0-0.005 *Hz* BandPass profile onto the unfiltered signal (*Figure 17*). Although the effect of the low-frequency components on the oscillations is much weaker than when the Subject was present, the displacement of the *COO* from the natural *COO* is still evident. Moreover, the magnitude of the Δ*COO* slowly diminishes toward the natural *COO*. The retention of these vibrational effects on the oscillations of the Pendulum for an extended period of time (more than 30 *min*) after the Subject departs is astonishing and must be accounted for.

Shifts in the magnitude of ΔCOO displacements kinetically resemble a chemical relaxation process

An important tool in the study of the mechanisms of chemical reactions involves perturbing an equilibrium-state chemical reaction using an external force that changes the position of the equilibrium. The chemical reaction will respond by moving toward the new equilibrium state. The rate at which the new equilibrium is approached conforms to a first-order rate law [1,2]

Equation 3 $A/A_0 = e^{-t/\tau}$

where A_0 is the initial displacement from equilibrium at $t = 0$, A is the displacement at time = t, and τ is the *relaxation time*. The physical significance of τ is that it is the time required to progress to 1/*e* of the way toward the new equilibrium position where *e* is equal to approximately 2.72. It is conceptually similar to the half-time of a reaction, except that instead of a (1/2-time), it is a (1/*e*-time).

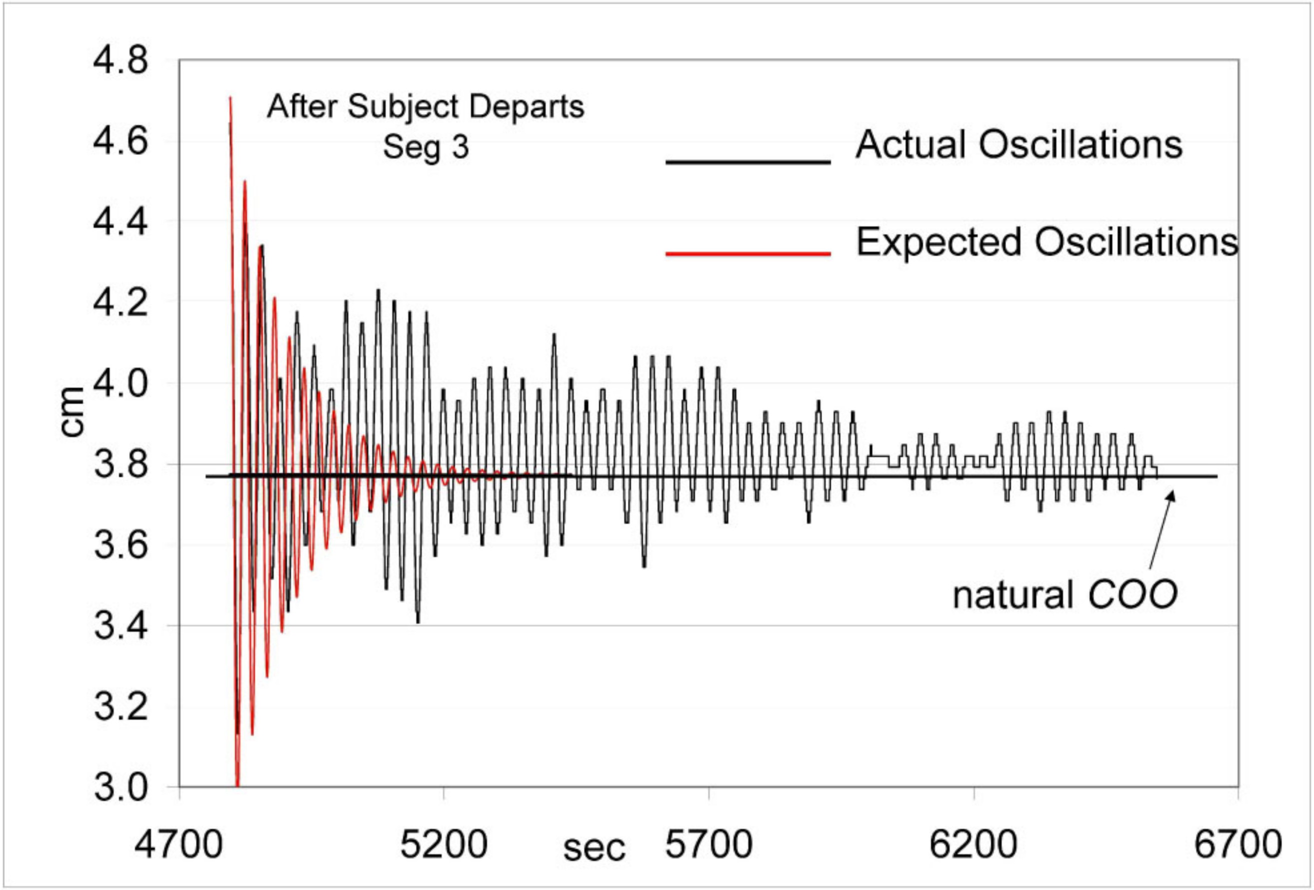

Figure 14. **Oscillation of the Pendulum when no Subject is present.** This is similar to *Figure 3*, except that the Pendulum oscillations are induced by successive puffs of air (see *Materials and Methods*), each of which is followed by a period of damping toward the natural *COO*. As described in *Results*, after each air puff, the Pendulum immediately reverts to classical damped *sho* behavior, with no residual effects being discernable. This is in contrast to after the Subject departs the Pendulum after *Seg 3* (*Figure 14*), in which substantial residual effects exerted by the Subject persist for at least 30 *min*.

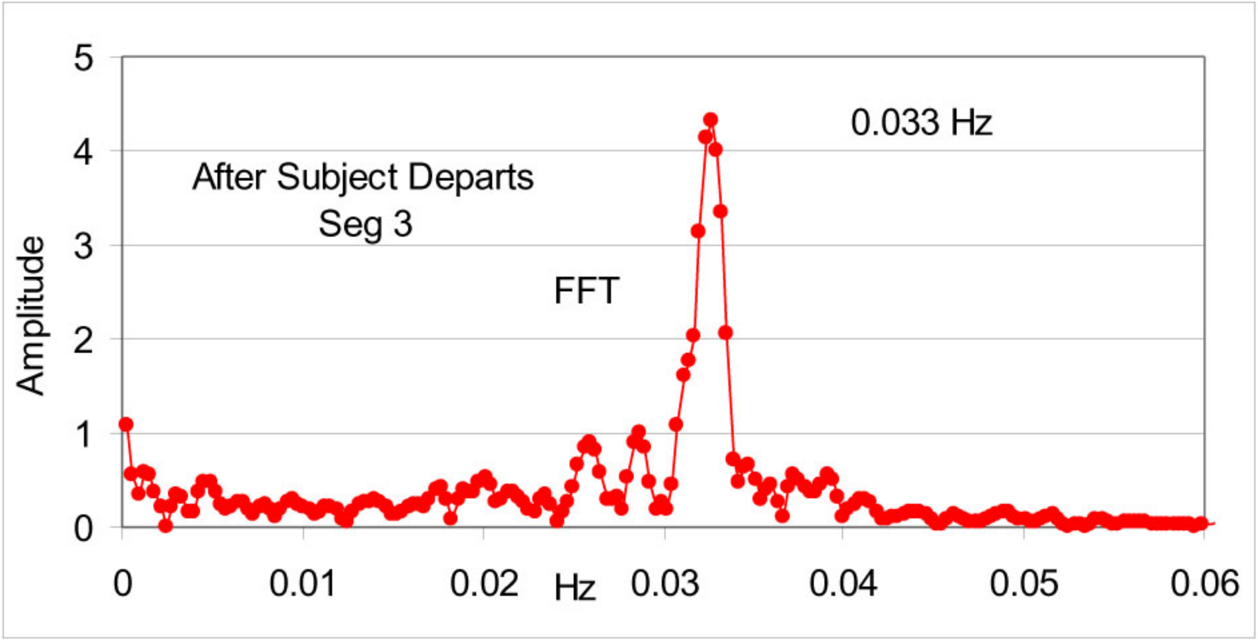

Figure 15. **FFT analysis of the post-*Seg 3* oscillations in *Figure 14***. To be compared to the FFT analysis of data in *Figure 3* in which no Subject was present. *Figure 15* shows a frequency peak at 0.033 *Hz*, which corresponds to the 0.034 *Hz* frequency obtained in the absence of a Subject. The major difference is that *Figure 15* shows many new frequencies that are absent from *Figure 3*. *Figure 16* shows these additional frequencies in greater detail.

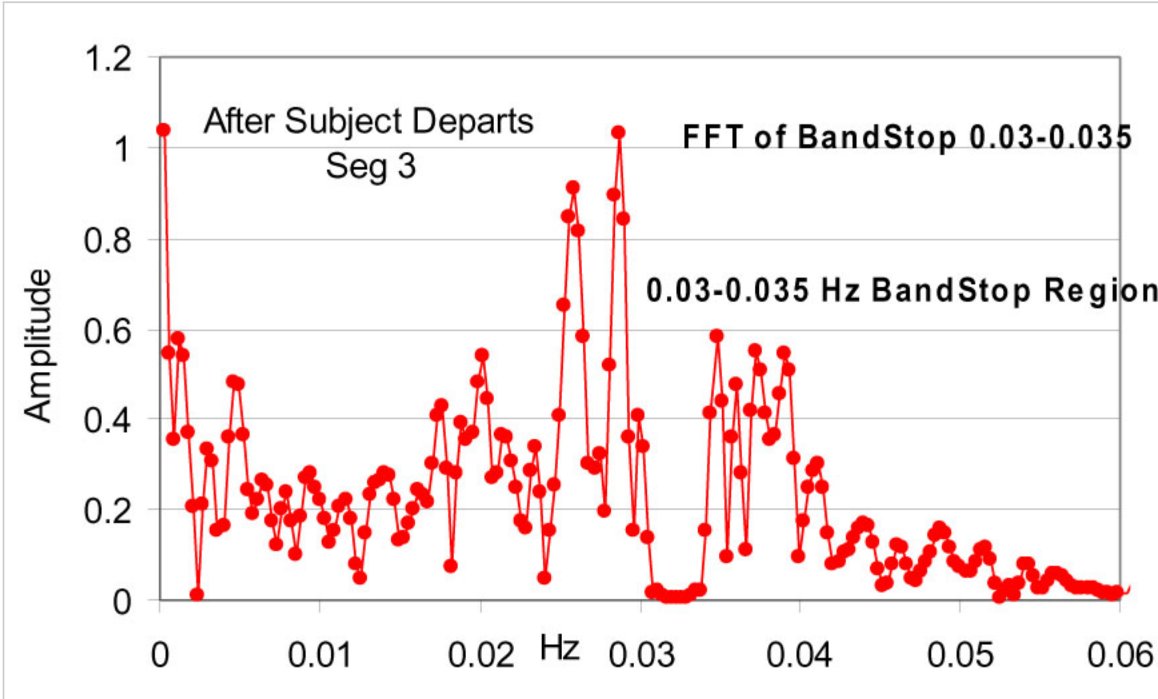

Figure 16. **FFT analysis of 0.03-0.035 *Hz* BandStop of *Figure 14* oscillations.** The 0.03-0.035 *Hz* frequency component was removed from the oscillation signal of *Figure 14*. *Figure 16* shows the FFT analysis of the remaining signal components. Many frequency components remain, as described in *Results*.

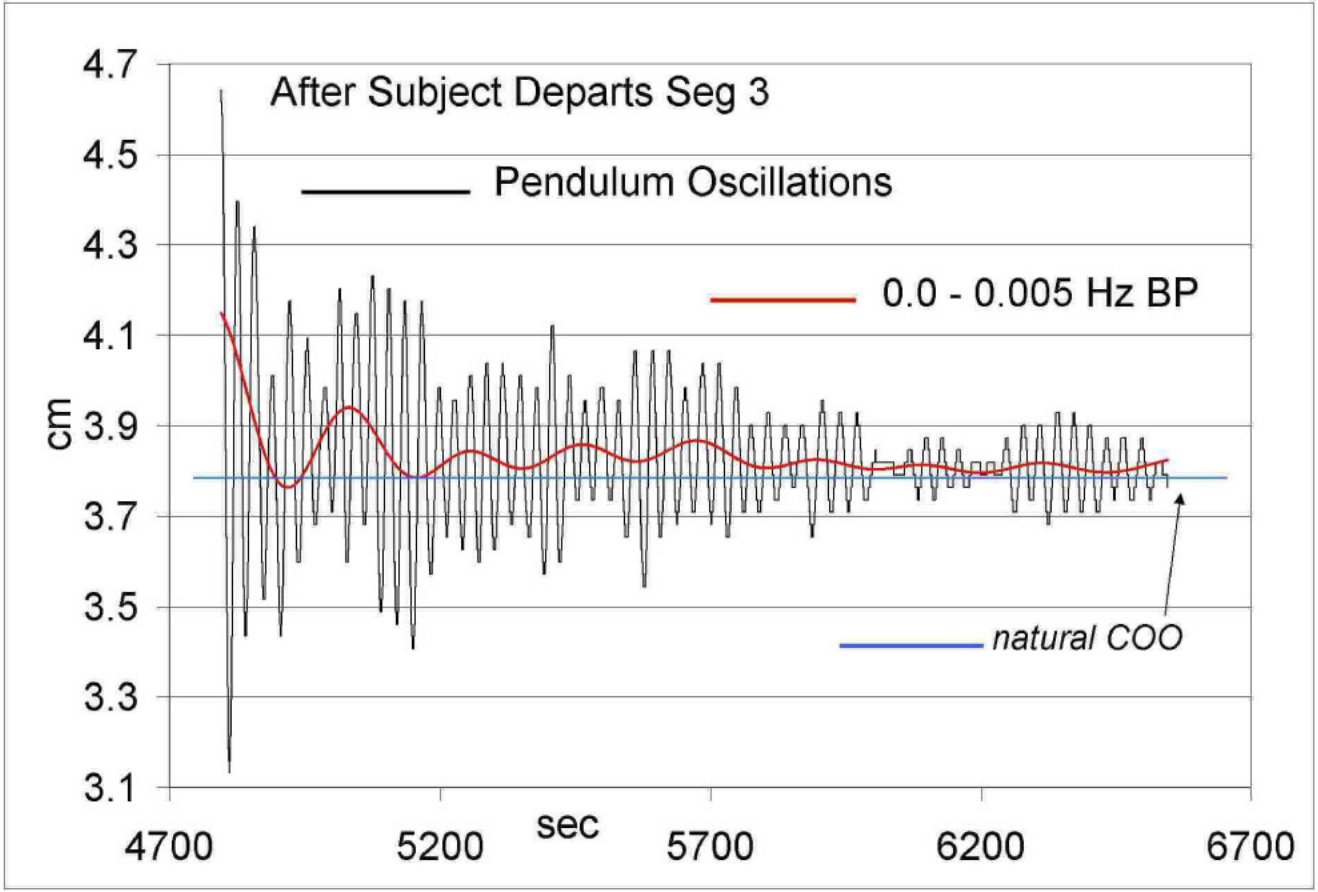

Figure 17. **Overlay of 0.0-0.005 *Hz* BandPass component onto the post-*Seg 3* oscillation signal from *Figure 15*.** *Figure 9* showed that low-frequency components are responsible for the deviations of the *COO* away from the natural *COO* when a Subject is present. A 0.0-0.005 *Hz* BandPass filter (which encompasses this low-frequency range) was applied to the post-*Seg 3* signal in *Figure 14* and overlaid onto the unfiltered signal. This 0.0-0.005 *Hz* overlay is the *red curve*. It is evident that that the post-*Seg 3* signal retains a significant amount of this low-frequency component, which is absent from the non-Subject control in *Figure 3*. Moreover, not only is this low-frequency component present, but a significant Δ*COO* persists throughout this region (see *Results*).

Figure 17 showed that when the Subject departs from the Pendulum, the oscillations progress from a displaced *COO* toward the natural *COO*. This corresponds to a situation in which a change in an external perturbing force results in a change from one equilibrium position to another, so it is appropriate to apply the concepts of chemical relaxation kinetics to analyze this process, as shown in *Figure 18*. Superimposed on the oscillation data is a theoretical chemical relaxation curve with a $\tau = 600$ *sec*, which closely fits the decay process, whereas curves with other relaxation times (*not shown*) fit the data less well.

That these data conform to the kinetics of a chemical relaxation process suggests the intriguing prospect that what we are observing during the transition from one equilibrium position to another is, in fact, a chemical reaction. Whereas a conventional view of a chemical reaction is that it involves the breaking of one set of bonds in the reactants and the formation of a new set of bonds in the products, a more inclusive view of a chemical reaction embraces any process that results in a change in the molecular structure of the reactant to become the product; this change is not necessarily limited to the breaking and forming of chemical bonds. For example, when "reactant" chlorophyll antenna molecules absorb photons, the "product" chlorophyll molecules are different because some of their electrons have moved to elevated quantum-energy states, but covalent bonds have neither been broken nor formed. What have changed are the quantum states of the electrons. In lieu of developing a list of possible changes in molecular structure that could be involved here, we will apply the idea that a molecular structure has changed if any of its quantum-energy states has changed. That is to say, the relaxation processes we are observing represent inter-conversions among quantum states, neither defining those states, nor the mechanisms by which their inter-conversions are achieved.

The relaxation time for the shift between equilibrium positions is variable

Figure 18 showed the kinetic pattern of the shift in oscillation of the Pendulum that occurs when the Subject departs, from which a relaxation time (τ) of 600 *sec* was obtained. We will now apply the same kinetic analysis to the data obtained when the Subject was under the Pendulum. At the beginning of *Seg 2* (*Figure 7*), the Pendulum is equilibrated near its natural *COO*. As soon as the Subject is seated, the Pendulum begins to shift toward a Δ*COO* of 2.2 cm. Shortly after it reaches this new plateau, it then drops back toward the natural *COO*. Consider the possibility that whatever "spirally-directed-force" is being exerted, it "switches on" for some period of time, during which the Pendulum moves toward the new equilibrium position, and then "switches off," whereupon the Pendulum moves back toward its natural *COO* equilibrium position. If these transitions represent shifts from one equilibrium position to another, they can be analyzed using chemical kinetics. Theoretical chemical relaxation curves are superimposed on the experimental data in *Figure 19*. The process occurring immediately after the Subject sits under the Pendulum, during which the *COO* shifts from the natural *COO* to a displaced *COO* of 2.2 *cm*, shows a τ of 200 *sec*, whereas the shift back toward the natural *COO*, while the Subject is still present, has a τ of only 35 *sec*. These are to be compared to after the Subject departs, which shows a τ of 600 *sec*. There is a nearly 20-fold discrepancy among these relaxation times, and assuming that relaxation times are important, providing an explanation of these discrepancies is also important. A variety of

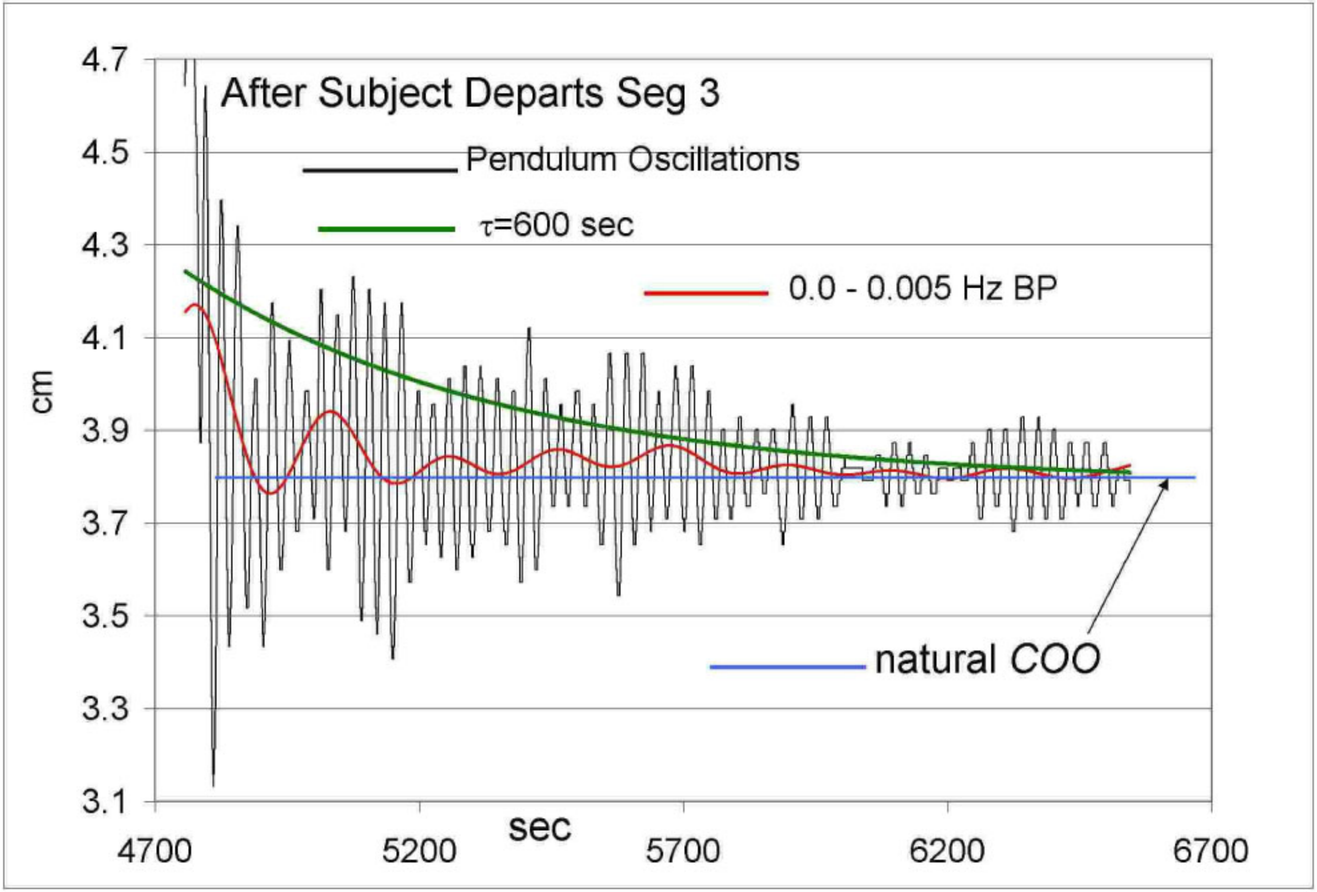

Figure 18. **The rate of approach of the post-*Seg 3* signal toward the natural *COO* corresponds to the kinetics of a chemical relaxation process.** The concepts of chemical relaxation processes and kinetics are described in *Results*. The *green curve* is a theoretical chemical relaxation process with a relaxation time of τ = 600 *sec* superimposed on the post-*Seg 3* signal data from *Figures 14* and *17*.

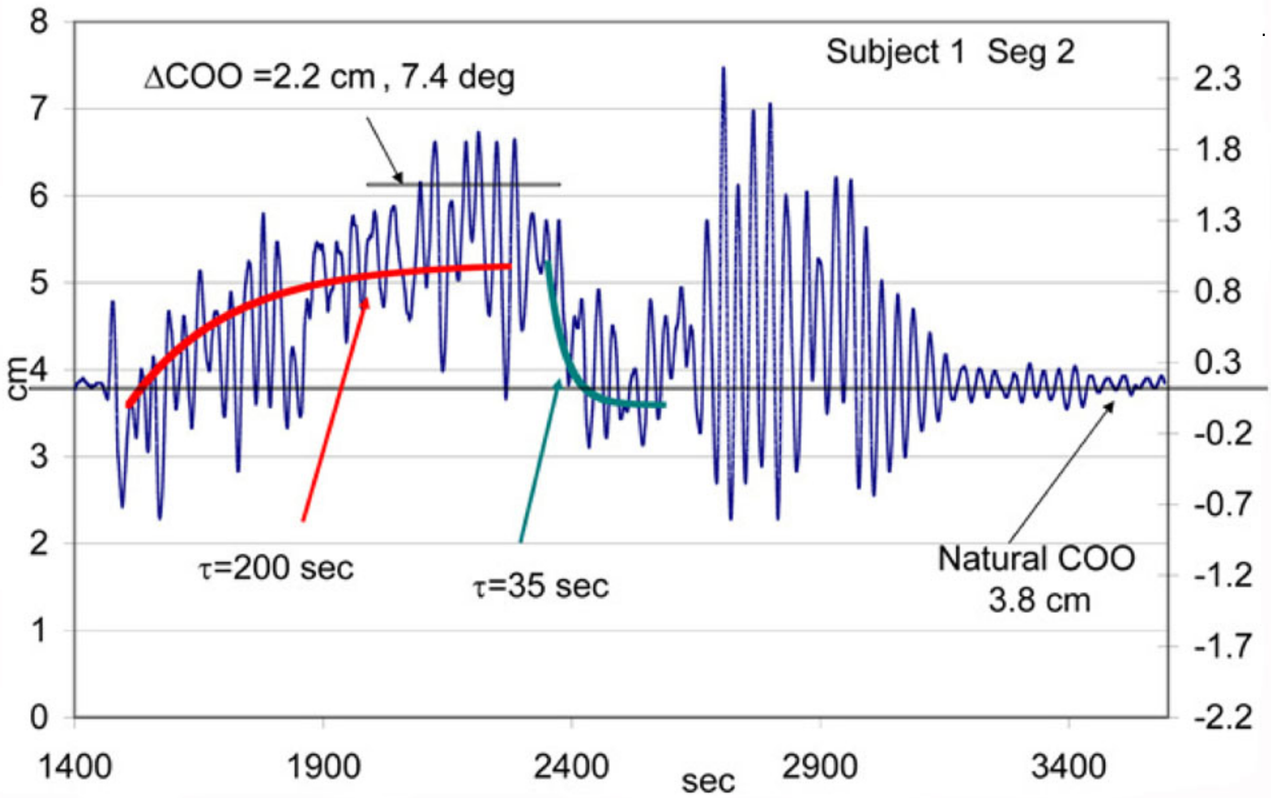

Figure 19. **Analysis of signal when Subject is present as a chemical relaxation process.** The signal data from *Seg 2* of *Figure 7* (when Subject 1 is present) is re-plotted here, and theoretical curves that represent chemical relaxation processes are superimposed on the signal. The *red curve* is a relaxation process with a relaxation time of τ = 200 *sec*, and the *green curve* is one with a τ = 35 *sec*, as described in *Results*.

conjectures and explanations will be presented in the *Discussion*. Of particular significance is that the relaxation rates in the presence of the Subject are more rapid than in the absence of the Subject.

Effects exerted by other Subjects

Several subjects have participated in these experiments. So far, no subject has failed to affect the Pendulum in a significant way, so we suspect that this ability is a universal human quality. Attributes that we consistently see are the abilities of a Subject to deflect the Pendulum away from its natural *COO*, to affect the amplitudes of oscillation of the Pendulum, and to induce new frequencies of oscillation. Whereas these attributes consistently appear with all Subjects, their strength and patterns differ. These are illustrated in experiments with Subject 2 and Subject 3. *Figure 20* shows a three-*Seg* experiment with Subject 2, and *Figure 21* shows a three-*Seg* experiment with Subject 3. Whereas Subject 1 (*Figure 7*) achieved a Δ*COOmax* of 2.2 *cm* (7.4 *deg*), Subject 2 achieved a Δ*COOmax* of 1.7 *cm* (5.7 *deg*), and Subject 3 a Δ*COOmax* of 1.6 *cm* (4.0 *deg*). On the other hand, Subject 3 showed the largest amplitudes, with amplitude swings of 6.5 cm (21 *deg*), whereas the largest amplitude swings of Subject 1 were 5.3 *cm* (17.6 *deg*), and those of Subject 2 were just 4.5 *cm* (14.9 *deg*). Subject 1 was an age 24-*yr* male medical student, Subject 2 was an age 66-*yr* male biochemist, and Subject 3 was an age 59-*yr* male astrophysicist. Subjects 1 and 2 had participated in many experiments prior to these, whereas this was the first experiment for Subject 3. Subject 1 is notable in having had several years of training in Eastern martial arts and meditative practices, so it is possible that the ability of Subject 1 to more dramatically displace the *COO* of the Pendulum may reflect these experiences. The experimental design we are using, in which the subjects can see the graphical data output during the course of the experiment, is suited to bio-feedback training, in which a Subject might learn how to consciously affect the motions of the Pendulum. It appears that Subject 1 may have already made progress toward this end, although it would take many additional experiments to confirm that bio-feedback learning is possible, which is beyond the scope of this paper. *Figure 22* shows the FFT analysis of all the *Segs* of the experiments with Subjects 1-3 so that the frequency variations can be compared. BandPass profiles of all the *Segs* (not shown) showed that the lowest frequencies (e.g., 0.0-0.002 *Hz*) that are related to the *COO* displacements are present in all of the profiles, as are a variety of higher frequencies. We note that there is as much variation among the frequency patterns exhibited by any of the individual Subjects as are the variations between Subjects.

Effects on the Pendulum *exerted by a Subject cannot be attributed to thermal/convective air currents*

A facile explanation of the response of the Pendulum to the presence of a Subject is that the Subject is a warm body that generates a variety of convective air currents, and that these air currents could be responsible for the anomalous Pendulum movements. A test of this idea is to place a heat source under the Pendulum and determine whether it can influence the Pendulum in a way that resembles what occurs in the presence of a Subject.

An electric cooking pot (Presto "Multi-Cooker" 6 qt Model 06003, 23 *cm* diameter, 26 *cm* high, clear glass lid, from target.com) was used as a heat source. The heat control

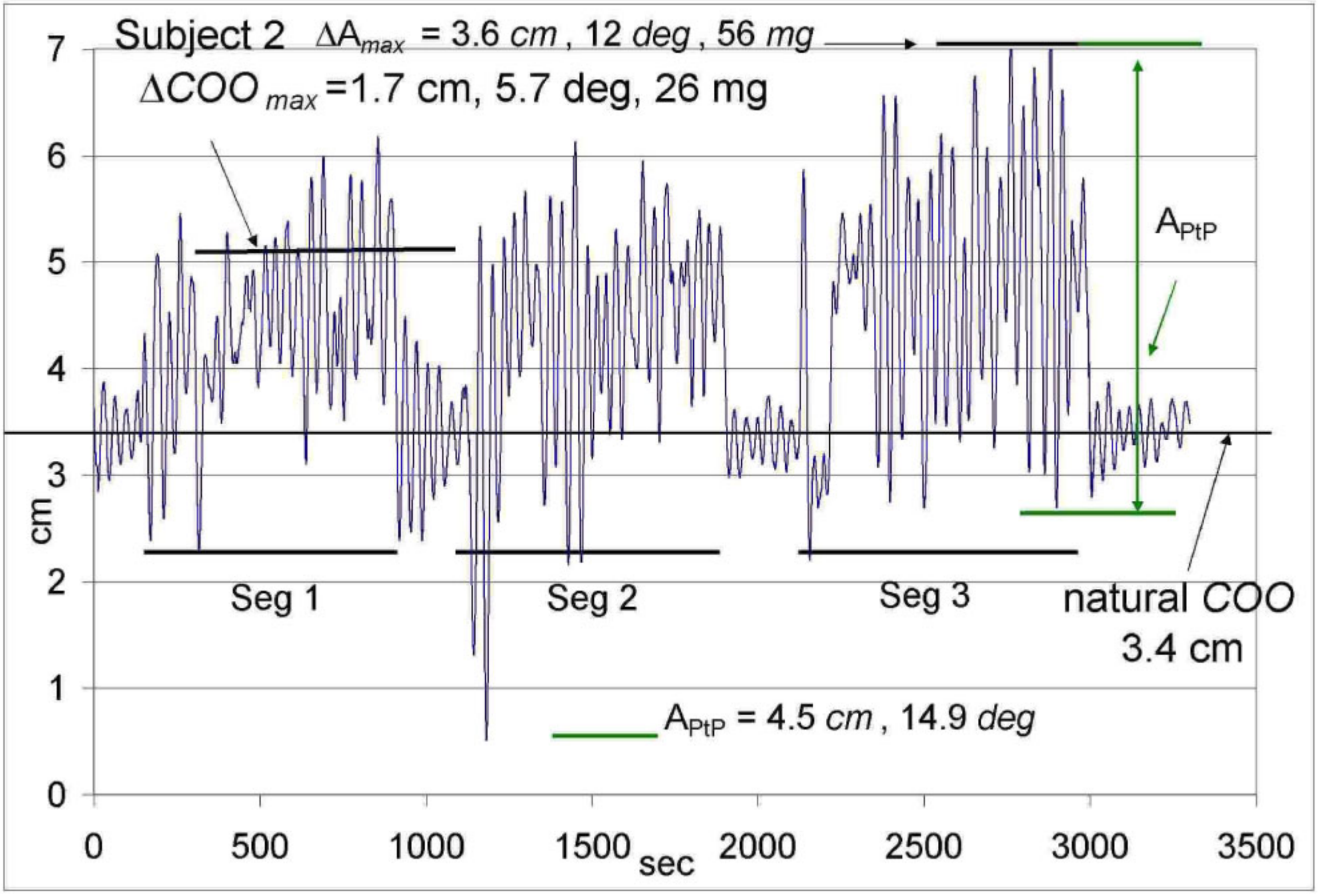

Figure 20. **A three-*Seg* experiment performed with Subject 2.** The initial seconds of the experiment are oscillations prior to Subject 2 being seated under the Pendulum. *Seg 1* is a period of time during which Subject 2 is seated under the Pendulum, as are *Seg 2* and *Seg 3*, respectively. When the Subject is present, the amplitudes of the oscillations and the Center of Oscillation (*COO*) of the Pendulum both change dramatically, with the maximum Δ*COO* expressed as *cm*, *deg* of rotation, and *mg* of force required to drive the rotation. A_{max} is the maximum amplitude of the displacement from the natural *COO* expressed as *cm*, *deg* of rotation, and *mg* of force. The vertical *green* arrow is the A_{PtP}, which is the largest peak-to-peak amplitude observed during the experiment, expressed as *cm* and *deg* of rotation. The results with Subject 2 can be compared with Subject 1 (*Figure 6*) and with Subject 3 (*Figure 21*).

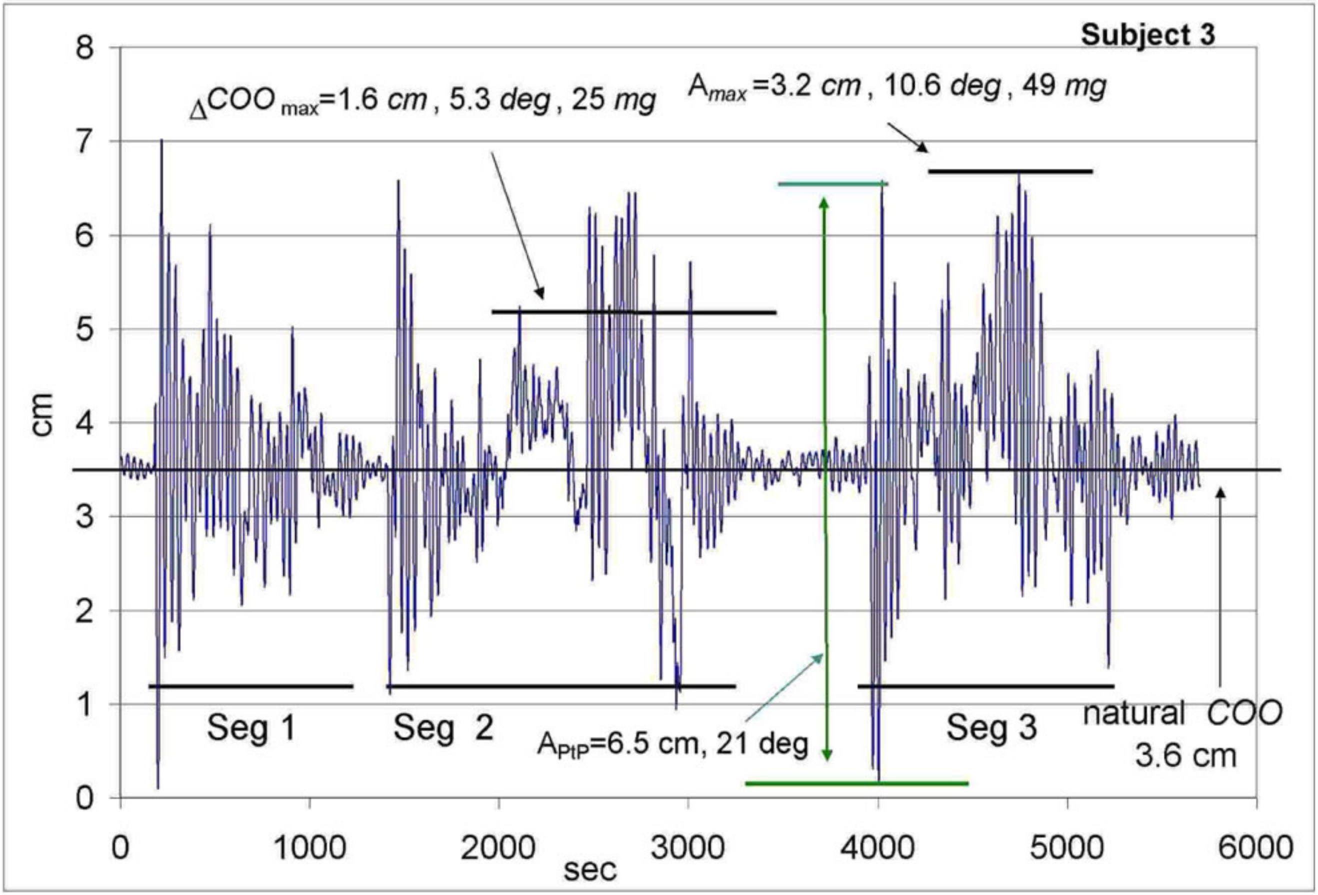

Figure 21. **A three-*Seg* experiment performed with Subject 3.** The initial seconds of the experiment are oscillations prior to Subject 3 being seated under the Pendulum. *Seg 1* is a period of time during which Subject 3 is seated under the Pendulum, as are *Seg 2* and *Seg 3*, respectively. When the Subject is present, the amplitudes of the oscillations and the Center of Oscillation (*COO*) of the Pendulum both change dramatically, with the maximum Δ*COO* expressed as *cm*, *deg* of rotation, and *mg* of force required to drive the rotation. A_{max} is the maximum amplitude of the displacement from the natural *COO* expressed as *cm*, *deg* of rotation, and *mg* of force. The vertical *green* arrow is the A_{PtP}, which is the largest peak-to-peak amplitude observed during the experiment, expressed as *cm* and *deg* of rotation. The results with Subject 3 can be compared with Subject 1 (*Figure 6*) and with Subject 2 (Figure 20).

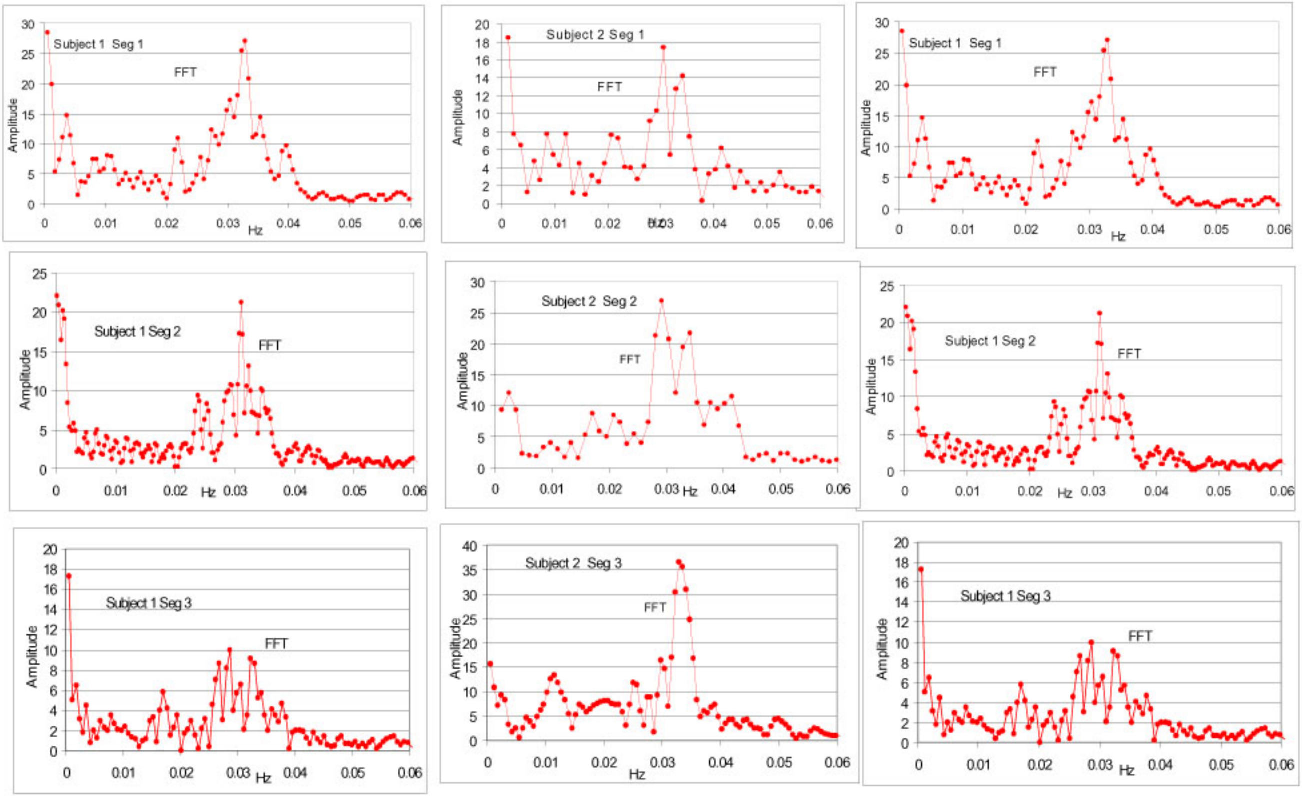

Figure 22. **FFT analysis of the oscillation signals obtained in all *Segs* of experiments with Subjects 1, 2, and 3.** The signal data of all of the *Segs* in *Figures 6, 20,* and *21* are subjected to FFT analysis, and the results compared in *this Figure*. *Segs 1-3* are vertically aligned for each Subject, as described in *Results*.

encompasses a 30-230^0C temperature range. The test was in two stages, the first being at the temperature of a Subject, and the second, at a temperature near the boiling point of water. Using a thermocouple (Vernier Model STS-BTA recording surface-sensor thermocouple, from vernier.com), the temperature immediately above a Subject's cranium was determined to be about 33^0C. An STS-BTA thermocouple probe was duct-taped to the bottom edge of the cooking pot, which is very close to the 1,500 W heating element. Another was duct-taped to the glass lid of the cooking pot, and another to the middle of the side of the pot. The pot was placed on a wooden platform under the Pendulum so that the lid of the pot occupied the same position that the cranium of a Subject would occupy. The pot was turned on, and the temperature control was adjusted so that the temperature of the glass lid of the pot was equilibrated at 33^0C. Monitoring the temperature of the lid for 1 *hr* ensured that equilibration was achieved. Although both the temperature of the lid and the side of the pot were a fairly constant 33^0C, the temperature of the bottom edge of the pot showed large variations (between 33 and 40^0C). This is due to the fact that the temperature of the pot is controlled by the temperature controller that switches the 1,500 W heating element on and off; while it is on, the bottom of the pot heats dramatically, and then drops dramatically when the element turns off. These temperature variations at the bottom of the pot should create heated air that would waft upward and affect the Pendulum. Although a Subject would not produce these temperature variations and the resulting thermal convection currents, the fact that the pot produces them allows an assessment of the effects of air currents of this magnitude. *Figure 23* shows the effects of the 33^0C cooking pot on the Pendulum. The very beginning of the experiment shows the Pendulum oscillating around its natural *COO*, whereupon the Pendulum was activated with a puff of air, followed by a damping process. The Pendulum was allowed to equilibrate at its damped state for about 1,000 *sec*. The temperatures of the three surface areas of the cooking pot during this entire period are superimposed on the Pendulum oscillations in *Figure 23*. Whereas both the lid of the pot and the middle of the side of the pot are maintained at a fairly constant 33^0C, the bottom edge of the pot shows temperature changes that are caused by the heating element cycling on and off at regular intervals, shifting back and forth from 33^0C to about 40^0C. The entire oscillation profile after the Pendulum has damped out is very quiet, but it is evident that when the heating element turns on, some tremors are introduced into the profile. We argue that these tremors caused by the temperature oscillations, although quite small, are larger than would be caused by any thermal air current generated by the Subject, whose temperature is as constant as the lid of the cooking pot. Furthermore, the 33^0C cooking pot did not induce changes in the *COO*. It therefore seems unlikely that the effects on the Pendulum are caused by the fact that the Subject is a moderately warm body. This is reinforced by the following experiment, in which the effect of a high-temperature cooking pot is studied.

We now look at the effect of the cooking pot when it is set at a high temperature, *i.e.*, 93^0C. The purpose of this high-temperature experiment is to intentionally create high-amplitude thermally-induced air currents that should have dramatic effects on the Pendulum. We can then determine whether these intentionally-induced air currents can cause the kinds of effects that are observed with the Subject; and especially whether these air currents can drive sustained displacements from the natural *COO* and amplitudes that are of magnitudes as great as or greater than those produced by the Subject. If the high-temperature air currents can produce these effects, one might expect that the magnitudes

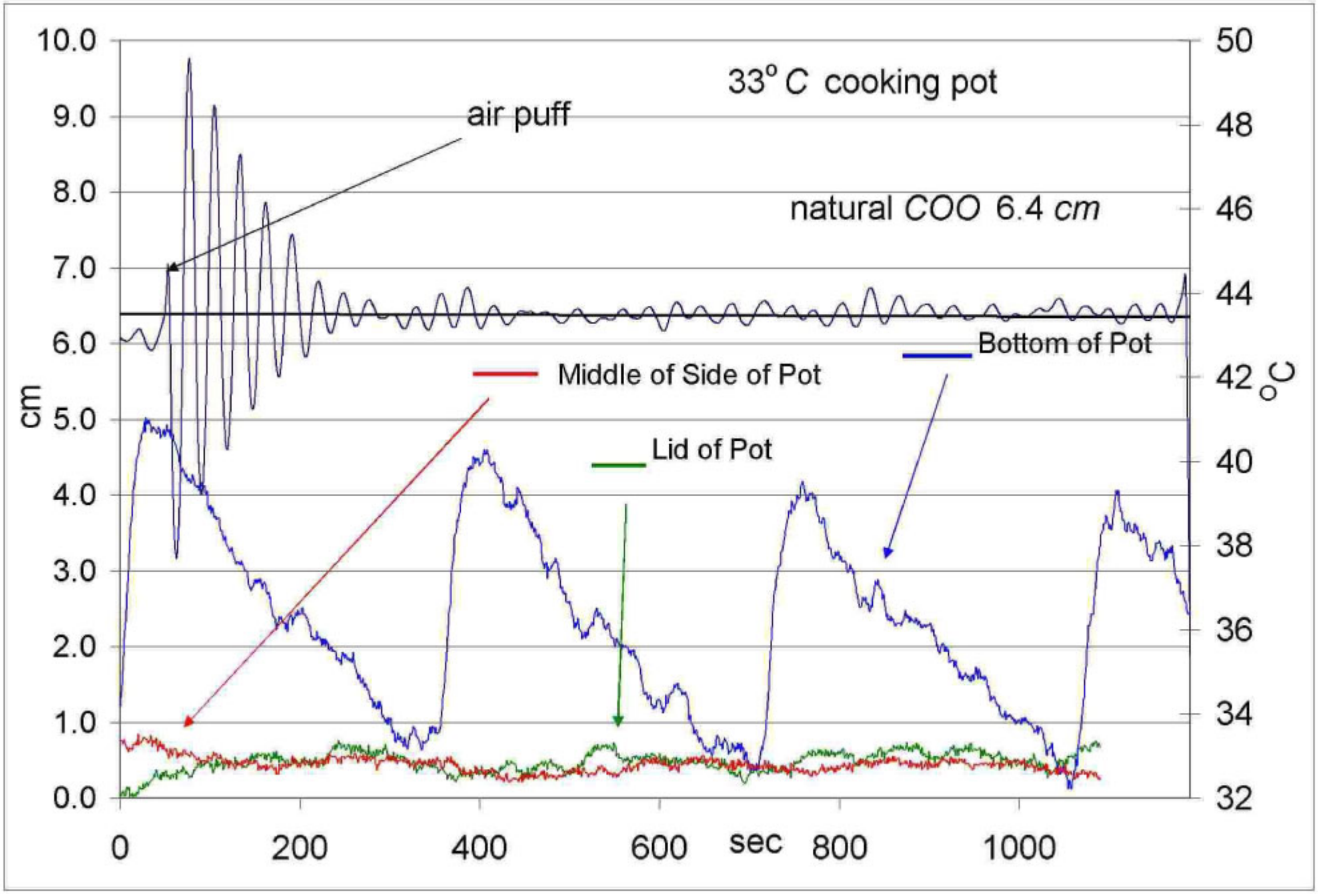

Figure 23. **Effects exerted on Pendulum by air currents generated by a cooking pot equilibrated at 33° *C*.** A cooking pot with a glass lid was placed under the Pendulum, equilibrated at 33° *C*, and the effects of resulting air currents on oscillations of the Pendulum are described in *Results*. The temperatures of different areas of the cooking pot were monitored with recording thermocouples, with the *blue curve* showing the temperature of the bottom edge of the pot (near the heating element), the *red curve* the temperature of the middle of the side of the pot, and the *green curve* the temperature of the glass lid of the pot. The *upper half* of the *Figure* shows the effects of the resulting air currents on the oscillations of the Pendulum.

of these effects would be much larger than could be produced by the Subject, who is at a much lower temperature.

Figure 24 shows the response of the Pendulum to the $93^{0}C$ cooking pot. In this experiment, the Pendulum is activated with a puff of air while the cooking pot is at *Room Temp*, about $24^{0}C$. The cooking pot, which had its lid removed to facilitate formation of turbulent air currents that are generated from the bottom of the pot, is then turned on at a setting that equilibrates at $93^{0}C$, and the effects of the ensuing turbulent air on the oscillations of the Pendulum are monitored over a period of about 2,000 *sec*. We note that the air currents created by the lidless $93^{0}C$ cooking pot are quite substantial, as estimated by holding one's hand above the Pendulum, which is constructed of porous steel mesh. The warm air currents that flowed through the Pendulum created a sensation similar to what is felt when holding a hand above a hot stove element. Some rocking motion of the Pendulum could be seen as it was buffeted by the air currents created at this high temperature. The $93^{o}C$ pot is so hot that touching it longer than a brief moment would inflict severe burns. We argue that if these turbulent air currents cannot duplicate the effects that are exerted by the Subject, then random thermal air currents, even those that are much stronger than could possibly be caused by a Subject, cannot explain our results.

Examination of the oscillation profile while the cooking pot is heating up, which it does very quickly, shows effects both on the amplitudes of oscillation, and deviations from the *COO*. Although these effects appear to mimic what occurs when a subject is under the Pendulum, analysis shows that they are actually quite different, both quantitatively and qualitatively. *Figure 24* shows that the amplitudes of oscillation increase immediately after the heat is turned on, which then increase in intensity until a maximum is reached at about 1,800 *sec*, whereupon the amplitudes of oscillation indeed become substantial. The very largest displacement, A*max*, from the *COO* is 2.9 *cm*, 9.6 *deg*, which corresponds to a force of 44 *mg*. The largest peak-to-peak amplitude swing is 5.4 *cm*, 17.8 *deg*. The magnitudes of both these parameters are smaller than what is observed among the Subjects. For example, Subject 1 (*Figure 6*) achieved an A_{max} of 3.8 *cm*, 12.6 *deg*, 59 *mg*; and Subject 3 (*Figure 21*) achieved an A_{PtP} of 6.5 *cm*, 21 *deg*, both of which are substantially greater than is achieved from the $93^{o}C$ cooking pot (Table I). Moreover, the Δ*COOmax* that is induced at this high temperature is just 20% of that induced by the *Subject* (Table I) and occurs over a much shorter time scale. The substantive conclusion is that the forces exerted on the Pendulum by a body-temperature Subject are substantially greater than the turbulent-air forces created by the near-boiling temperature cooking pot, and that those forces behave completely differently than those induced by the Subject. These observations lead us to conclude that the effects of the Subject on the Pendulum could not possibly be caused by thermal air currents induced by the Subject. The only other sources of turbulent air from the Subject that we can think of are breathing and body motions. These are ruled out by several experiments (not presented here) in which the Subject stopped breathing for at least 1 *min* while sitting very quietly during times in which the Δ*COO* was large, whereupon the Δ*COO* did not diminish in response.

This conclusion is further supported by analysis of the oscillation frequencies of the Pendulum that are induced by the $93^{o}C$ cooking pot. *Figure 25* shows the FFT of the oscillation signal in *Figure 24* during the time when the cooking pot is on. The *Figure 24*

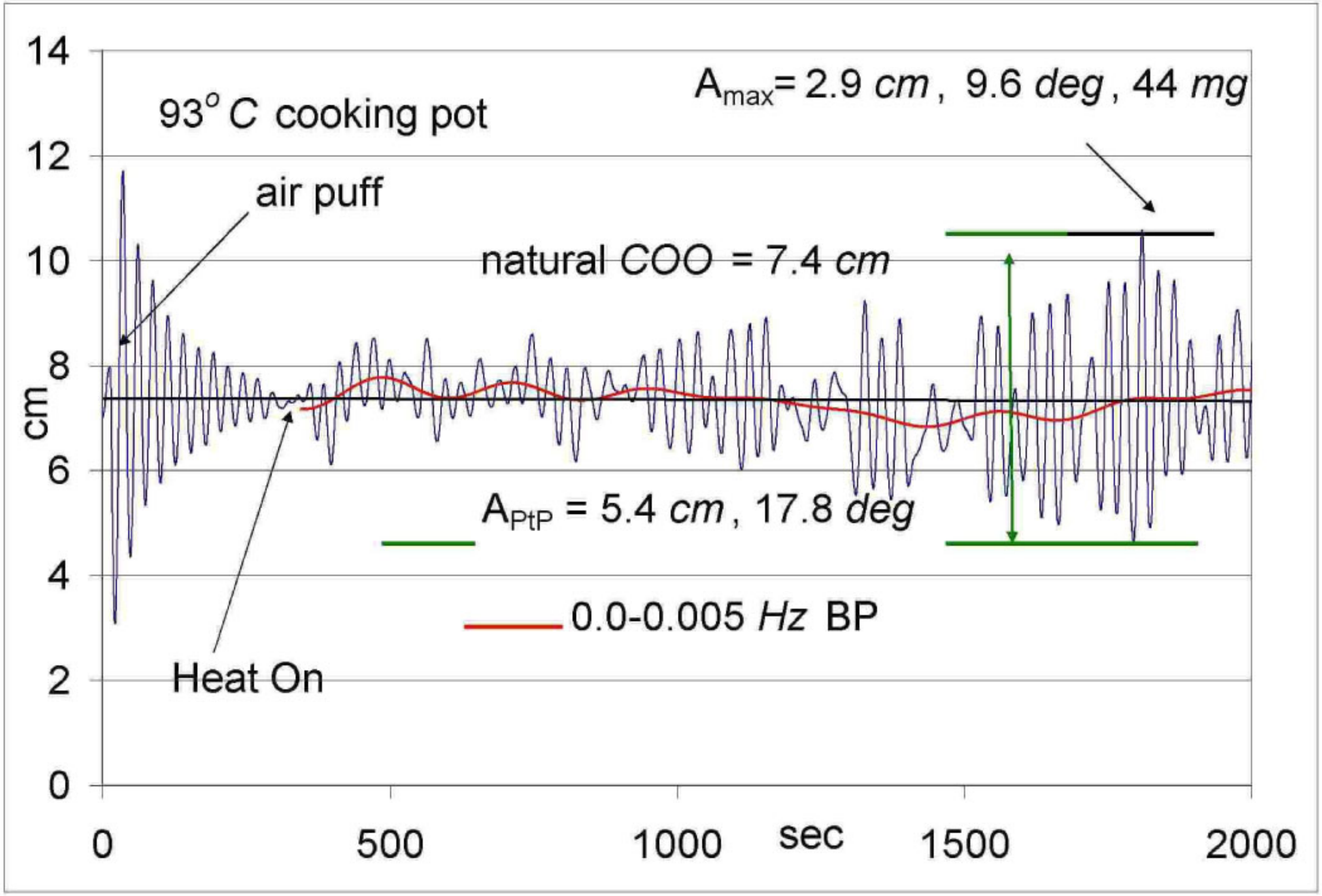

Figure 24. **Effects exerted on Pendulum by air currents generated by a cooking pot at 93° *C*.** A cooking pot without a lid was placed under the Pendulum, and then turned on at a temperature setting that equilibrates at 93° *C*, and the effects of resulting air currents on oscillations of the Pendulum are described in *Results*. The Pendulum was activated with an air puff when the pot was at room temperature, and after 400 *sec* of damping toward the natural COO, the cooking pot was turned on, and the effect of the resulting air currents were monitored for 1,600 *sec*. A_{max} is the maximum amplitude as measured from the natural *COO*, expressed as *cm*, deg, and *mg* of force. A_{PtP} is the largest peak-to-peak amplitude that was observed during the experiment, expressed as *cm* and *deg* of rotation, as described in *Results*. The *red curve* is a low-frequency (0.0-0.005 *Hz*) BandPass profile of the signal data obtained with the pot was on, superimposed onto the unfiltered signal.

Table I. Effects of Subjects *vs*. Controls on Amplitudes and ΔCOO

	A*max*	$\mathbf{A}_{PtP}$	$\Delta COOmax$
Subject 1	3.8cm	5.3cm	2.2cm+
Subject 2	3.6cm	4.5cm	1.7cm+
Subject 3	3.2cm	6.5cm	1.6cm+
33^oC Cooking Pot	0.2cm	~0.6cm (@ 390sec)	~0
93 ^oC Cooking Pot	2.9cm	5.4cm	<0.6cm +/-

Legend to Table I. Effects of Subjects on Pendulum motions compared to the effects of control sources of heated thermal air currents. **A*max*** is the largest amplitude as measured from the natural *COO*. $\mathbf{A}_{PtP}$ is the largest amplitude displacement measured as the total peak-to-peak displacement of a single swing of the Pendulum. **Δ*COO*** is the magnitude of displacement away from the natural ***COO*** during any particular swing of the Pendulum. **Δ*COOmax*** is the largest **Δ*COO*** that was observed during the experiment. *See text* for further details.

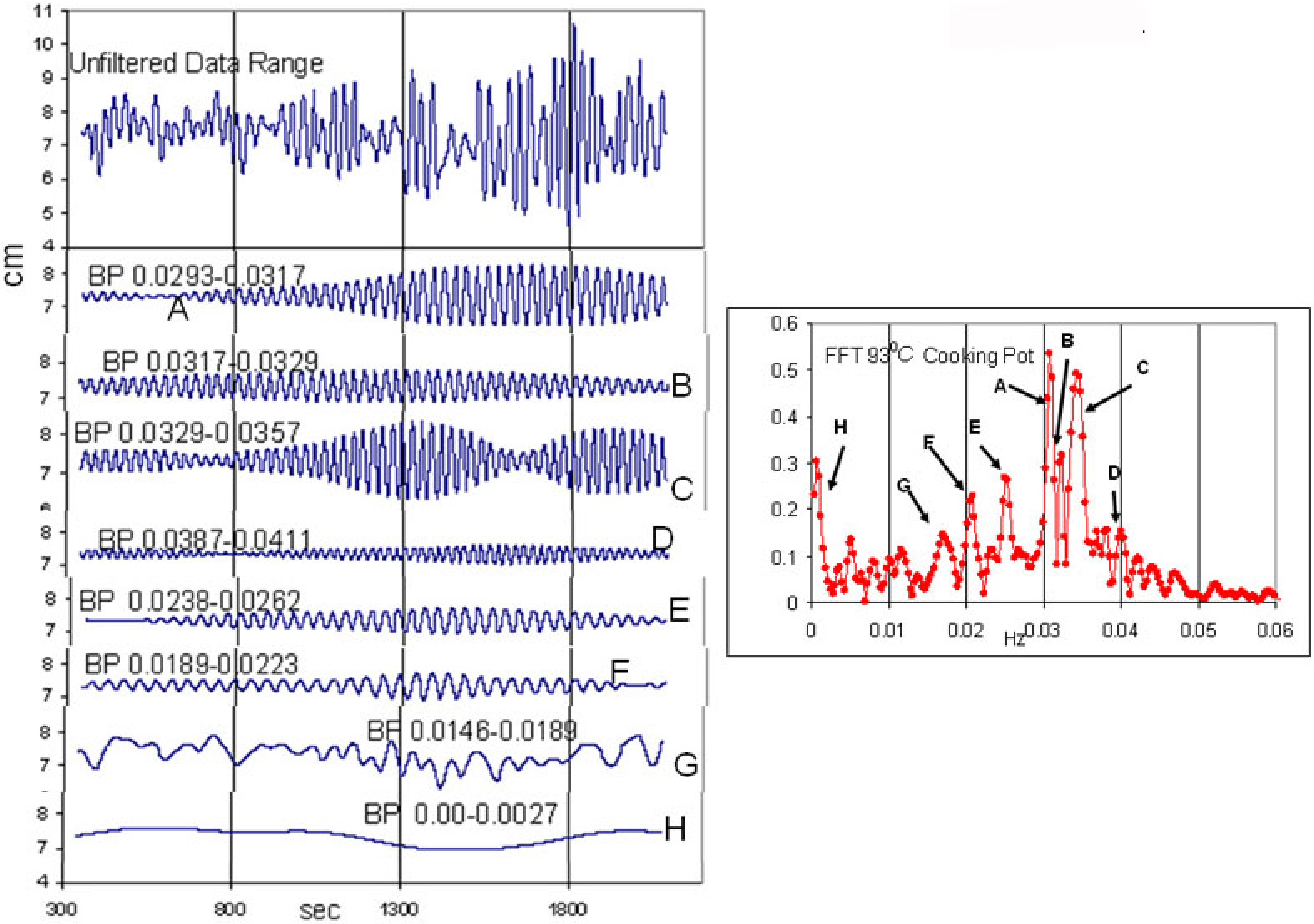

Figure 25. **Frequency components that contribute to the oscillation profile caused by high-temperature air currents.** The *right half* of the *Figure* is the FFT analysis of the oscillation signal (*Figure 24*) of the Pendulum as it is buffeted by the high-temperature air currents created by the lid-less cooking pot at 93° *C*. The *top-left panel* shows the unfiltered oscillation signal from *Figure 24*. The unfiltered signal was subjected to several BandPass filters, each of which extracted a selected frequency range from the unfiltered signal. The results of these various filters are shown as *curves A-H* in the *left panel*, *e.g., curve A* is the result of a 0.0293-0.0317 *Hz* BandPass filter. This filter range corresponds to the frequency range from the *left minimum point* of *peak A* of the FFT spectrum, to the *right minimum point* of *peak A*; and so on for curves B-H. *Curve H* corresponds to the *red curve* that is superimposed on the oscillation signal in *Figure 24*, as described in *Results*. *Curves A-H* accordingly show the contribution of each respective frequency range to the oscillation profile of the unfiltered data (*top left*). The *cm* scale is the same for all the *A-H* curves, so the magnitudes of all the frequency components are measured on the same relative scale, *i.e.*, the apparent relative magnitudes of all the *curves* in the *left panel* are the same as the actual relative magnitudes.

amplitudes and the *Figure 25* FFT profile show a superficial resemblance to the *Seg 2* oscillation signal profile of Subject 1 (*Figure 7*), and its FFT profile in *Figure 8*. The FFT profile of the 93^{o} *C* data shows many new frequencies, just as the FFT profile of the Subject 1 data shows many new frequencies. What is completely different is the qualitative nature of the frequencies that contribute to the two FFT profiles. The frequency analysis of the Subject 1 FFT (*Figure 10*) shows that all the major frequencies show undulating patterns that wax and wane in intensity, with many peaks and troughs among them. In contrast, the frequency analysis of the 93^{o}*C* oscillation signal (*Figure 25*) shows many fewer undulations, with *curve C* of *Figure 25* being the only one with significant undulations. It is possible that the 93^{o}*C* temperature of the cooking pot is so extreme that the nylon fiber that supports the Pendulum heats up during the experiment, which would result in a change in the *torsional constant* (κ) of the fiber. If this were to occur, it should shift the natural frequencies of oscillation, which should in turn decrease the magnitude of these frequencies. *Figure 25* does not show much evidence of such frequency shifts, which is in contrast to *Figure 10* in the presence of the Subject that shows suppression of the natural frequencies of the Pendulum. These differences contribute to the idea that the effects of forces exerted on the Pendulum by a Subject are completely different from the effects of forces that are exerted by thermal air currents.

This is especially evident in *Profile H* of *Figure 25*, which is the 0.0-0.0027 *Hz* BandPass frequency component of the *top panel* frequency signal. This is the frequency component that contributes to the large Δ*COO* of the Subject 1 oscillation signal in *Figure 9*. Superimposing this low-frequency component (*red curve*) onto the oscillation signal in *Figure 24* shows that the deviations from the natural *COO* are quite small, and that the deviations oscillate between positive deviations and negative deviations, as would be expected from the effects of thermal air currents that would be impinging from random directions.

We conclude that the effects of thermal air currents on the Pendulum are both qualitatively and quantitatively quite different from the effects on the Pendulum that are exerted by a Subject. Particularly impressive is the observation that a 93^{o}*C* cooking pot that generates strong thermal air currents cannot affect the motions of the Pendulum as strongly as can a Subject sitting under the Pendulum.

Discussion

We are now at the stage of the scientific process at which we have performed experiments that suggest the discovery of a previously-unrecognized form of energy in the vicinity of a human Subject that strongly affects the motions of a simple torsional pendulum. We have been diligent in eliminating experimental artifacts and we are convinced that our results reflect actual phenomena. We therefore report these results together with a description of the experimental design in sufficient detail that others can reliably repeat our experiments and confirm that our methods and data are valid. Because our results are so unexpected, it is a challenge to provide explanations for them. Good data do not automatically lead to good interpretations, so we expect to make errors in our hypotheses; but additional experimentation, especially by others who are skeptical of our data and interpretations, will quickly falsify those ideas that are incorrect, and lead toward more robust alternatives. For the scientific process, it is less important that a hypothesis be correct than that it inspire experiments designed to test it.

We begin our interpretation with the origin of the energy produced by the Subject that causes the Pendulum to deviate from its natural ideal behavior, to oscillate with many new frequencies at high amplitudes and to shift away from its natural *COO*. We see two possibilities. One is that the energy originates from the metabolic energy of the Subject, and there is an energy-transduction process that converts metabolic energy into the form of energy that affects the Pendulum. The other is that the energy is derived from the environment, with the Subject possessing the ability to collect the energy and transduce it into a form that affects the Pendulum. Of the two, we prefer the first, in which the energy is derived from the metabolic energy of the Subject.

Biological energy-transduction processes are notoriously complex, examples being photosynthesis and oxidative phosphorylation. These processes occur in specialized organelles, such as chloroplasts and mitochondria, which have evolved their functions over millions and even billions of years. A logical candidate to perform the energy-transduction observed here is the neuron, which is even more specialized and highly evolved than chloroplasts and mitochondria, in that neurons are regarded as the origin of consciousness and the intellect, and as the repository of memories. The forces of natural selection necessary to drive the evolution of complex energy-transduction systems would not occur unless they were highly advantageous to survival. This suggests that the energy that alters the oscillations of the Pendulum is as crucial to our survival as the ATP that is synthesized by our mitochondria. If so, our being oblivious to this energy is a barrier to our ability to comprehend our fundamental nature.

We speculate as to the mechanism by which the energy produced by the Subject induces altered motion of the Pendulum. We are reminded of Einstein's "spooky action at a distance," a phrase he used to describe quantum entanglement between particles, in which a change in one of them instantaneously results in a change in the other, no matter how far apart they are. The behavior of the Pendulum in the presence of a Subject looks like "action at a distance," so quantum entanglement could play a role.

To gain insight into the mechanism, we review what was presented in the *Results*. One observation was that the presence of the Subject caused the Pendulum to deviate dramatically from its natural *COO*, and to oscillate at this Δ*COO* for substantial periods of time, *e.g.*, 10-15 *min*. This implies that the Subject provides a driving force to the Pendulum, and that the force exerted by the Subject is at least partly in the form of a "spinning vortex," although other aspects of the force appear more as "bursts" that enhance the amplitudes of the Pendulum oscillations at non-natural frequencies without necessarily altering the *COO*. Another observation was that the deviation from the natural *COO* and the induction of new frequencies did not immediately abate when the Subject left the Pendulum. Instead, the intensity of these effects decreased gradually, with kinetics resembling a chemical relaxation process involving a shift from one equilibrium position to another, with the final position being the natural *COO* and the natural frequency of the Pendulum. The relaxation time, τ, for the approach to the natural behavior of the Pendulum was about 600 *sec*. This contrasts dramatically with apparent relaxation times that were obtained when the Subject was under the Pendulum. Then, the Pendulum began to shift toward a displaced *COO* soon after the Subject was seated under it. The τ for this shift in the equilibrium position was 200 *sec*, and this shifted equilibrium position was sustained for 10-15 *min*. For reasons that are unclear, the Pendulum then returned toward the natural *COO*, and when it did so, had a relaxation time of τ = 35 *sec*. Both of the relaxation rates in the presence of the Subject are much more rapid than after the Subject left the Pendulum, *i.e.*, there is nearly a 20-fold difference among the rates. It can therefore be stated that the rate at which transitions are made from one equilibrium position to another is more rapid when the Subject is present than when the Subject is absent. Since we are biochemists, we gravitate toward the truism that in biological systems, the acceleration of reaction rates is due to catalysis by enzymes. Although we are not describing how it might occur, we argue that the more rapid relaxation rates toward a new equilibrium position in the presence of the Subject are the result of enzymatic catalytic processes coupled to an energy source. After the Subject departs, this catalysis ceases, whereupon subsequent changes in the Pendulum oscillations are spontaneous uncatalyzed reactions which are disconnected from the energy source, and therefore equilibrate back toward the un-energized state.

We ordinarily think of catalysis as resulting in an increase in the rate at which chemical reactions reach equilibrium. In the case of enzymes, the rate increase is primarily due to a reduction in the activation energy required to reach the high-energy transition-state of the reaction. Enzymes are capable of establishing a transition-state that can be reached by an input of activation energy dramatically lower than that required by the non-enzymatic reaction. In most enzymatic reactions, the catalytic effect is limited to the rate at which equilibrium is achieved, and cannot affect the equilibrium position. However, in a subset of enzymatic reactions, such as the remarkable ATP synthetase [3] of mitochondria, a dramatic shift in the equilibrium position is possible if a coupled source of external energy is available. In the case of ATP synthetase, this source of external energy is the proton gradient. It is therefore reasonable to consider the possibility that the enzymatic reactions that drive the motions of the Pendulum can shift the equilibrium position of the Pendulum, if they are coupled to a suitable energy source.

Furthering this reasoning, we consider the idea that the novel motions of the Pendulum are the result of chemical reactions catalyzed by enzymes, and that these reactions are energetically coupled to the metabolic energy of the Subject. Clearly, these reactions would have to originate within the cellular structure of the Subject, perhaps within neurons. A product of these reactions might possibly be a molecular entity with a novel ability to become energetically entangled with surrounding molecules, which could induce them to undergo a change in molecular structure/quantum state that is related to the change in molecular structure/quantum state of the primary enzymatic product. We are thinking in terms of the classic “allosteric effect,” also called the “cooperative effect” in which a conformational change in a protein subunit drives adjacent subunits to undergo complementary conformational changes; examples being hemoglobin, aspartate transcarbamoylase, and the MAP-kinase signal-transduction proteins. We suggest that the difference here is that the change in molecular structure/quantum state is being communicated not only to immediately adjacent molecular structures, but to structures that are in another part of the cell, or in another cell, or even within an object, such as the Pendulum, that is separated from the primary molecular/quantum-state change by a substantial physical distance. The only mechanism we can think of to account for this is some form of quantum entanglement, by which the product of an enzyme-catalyzed intracellular reaction can become quantum-entangled with surrounding molecular structures, and thereby influence their behavior. Since quantum entanglement can be communicated among entities that are widely separated, the fact that the Subject is separated from the Pendulum by a substantial distance would not be a barrier to their interaction.

We now consider the possibility that all entities in the universe exist in a state of weak quantum entanglement, so that a weak entanglement interaction between Subject and Pendulum always exists; and that quantum-state products of certain enzymatic reactions within cells are able to intensify this already-established entanglement, so that the effects of entanglement are stronger than they would otherwise be. This is analogous to the enzymes of intermediary metabolism, which do not invent new chemical reactions, but rather selectively accelerate only those already-available chemical reactions that are essential for the cell's survival. It is as if those reactions not accelerated by enzymes do not exist, which causes the enzyme-accelerated reactions to dominate over all others, as is necessary for intermediary metabolism to function. Since all matter consists of waves, we think it likely that the underlying mechanism that could enable intensification of quantum entanglement between physically-separated entities would be some form of resonance coupling.

One might ask how an ability to intensify entanglement could evolve. Discoveries in biology during the last century are replete with examples of how biological evolution discovered solutions to problems that were not previously known to exist, and many modern technological advances have been inspired by studying nature's solutions to these problems. Studies of a variety of biological processes have established that quantum mechanics and quantum entanglement play important roles. For example, there is strong evidence that quantum entanglement is involved in the nearly-perfect efficiency by which photosynthesis transduces photon energy into chemical energy [4,5]. The mechanism by which olfactory receptors transduce the structures of odorant molecules into particular odors is attributed to quantum-mechanical processes [6,7]. Quantum entanglement has been implicated in consciousness, perhaps mediated by the microtubules present in neurons [8-11]. Some enzymes may have implemented quantum processes as a way to employ coupled nuclear quantum tunneling to enable an otherwise energetically-unfavorable enzymatic reaction to occur [12]. Recent studies suggest that the effects of entanglement on photons are retained long after the entanglement is broken [5,13]; this is consistent with the Pendulum retaining residual effects after the Subject has departed.

Photosynthesis evolved well over a billion years ago, and the fact that photosynthesis exploits quantum entanglement establishes a benchmark in time, which means that evolution must have exploited quantum entanglement well before that, and has been able to continue exploiting it ever since. A billion years is a long time to evolve survival strategies, and if it is possible for quantum entanglement to contribute to the evolution of consciousness, intelligence, and the ability to form and recall memories that has occurred during the last billion years, it likely would have done so. It is possible that these qualities evolved in tandem with the ability of the Subject to produce a form of energy that can interact with the Pendulum and affect its motions. We have argued that this would require the participation of a complex and therefore highly-evolved energy transduction system, which implies that it makes a significant contribution to our ability to survive. We acknowledge that our proposal that quantum entanglement plays a key role in this system represents a significant departure from well-established principles and well-understood processes. However, we point out that this is in response to experimental observations that represent a dramatic departure from anything that has been observed before, as far as we know. If we could propose a simpler explanation, we would, but we cannot think of one.

We believe that the Pendulum, or modified forms of it, will provide a means to explore the underlying mechanisms that enable a Subject sitting under the Pendulum to affect its motions. How this ability contributes to our fundamental nature, and how and why evolution has forged the difficult path to this end, are questions to investigate. For the answers to unfold, it is first necessary for others to repeat our experiments to confirm the suitability of our experimental design and the validity of our experimental results.

Ethics

Signed informed consent statements were obtained from all subjects.
The ethics committee that approved this protocol was the Institutional Review Board (IRB) of the University of Maryland, College Park.

Materials and Methods

Compressed air used to activate the Pendulum was from a can of #OM96091, 10 oz size, "gasduster" obtained from OfficeMax fitted with the included plastic extension tube to direct a controlled puff of air toward the outer edge of the Pendulum in the direction of its motion.

Figure 1 shows the Pendulum with a Subject seated under it. Photographs of the Pendulum components are in Figure 2. The dome-shaped energy collector is a Model #97061 14 *in* steel mesh food cover (black) that is 15 *cm* high and 34 *cm* in diameter, imported by LB International (lbimports.com); but available from a variety of on-line vendors. The plastic handle was replaced by a steel eye-bolt to which a nylon monofilament (M1430, 30-*lb*-test South Bend fishing line, Northbrook, IL) was tied. The other end of the filament was tied to another steel eye-bolt that was bolted to a support beam that was in turn attached to a heavy-duty camera tripod (Sunpak Model 7500 Pro) obtained from bestbuy.com. The length of the monofilament between the attachment knots was 1.7 *cm*. The knots used were "double half-hitch knots" which gripped the steel eye-bolts very tightly. The support beam was a 90 cm-long 3 *mm* thick aluminum angle beam (1.9 x 1.9 *cm* legs) with the tripod attachment point in the middle. A stabilizing counter-weight was placed on the side of the beam opposite from the Pendulum, which reduced stress on the tripod attachment and contributed to the stability of the Pendulum. The counterweight consisted of a 1.9 *l* plastic bucket with handle and lid (Rubbermaid Seal & Save) that contained 17 steel washers of the type shown in *Figure 2* and had a total mass of 806 *g*. The position of the counterweight was adjusted by sliding it to a position on the beam so that the stress on the tripod mounting was neutral. This counterweight was especially useful when weights were added to the dome collector in order to determine the torsional constant (*Figure 5*) of the suspending fiber. When in use, the Pendulum was adjusted with its lower edge about 2 *cm* above the eyebrow ridge of the Subject, as illustrated in *Figure 1*. At no time during an experiment did the Subject come in contact with the Pendulum.

Data collection and analysis were performed on a Windows XP computer with a 2.8 *GHz* Pentium D CPU processor and 1 *GB* of RAM. Programs used for data analysis and presentation were Microsoft Excel XP and PowerPoint. Motions of the Pendulum were monitored using real-time video object tracking of a target placed on the Pendulum. The target on the Pendulum was a 1 *cm* white dot on a black background, printed on standard copy paper using a HP LaserJet model 3500 color printer. While the Pendulum oscillated, the only thing that changed in the video image was the position of the white dot. An object tracking program written in LabView (National Instruments Graphical Programming Language) was used to locate the center of the white dot, as well as its diameter, both measured in pixel units of the image. The location of the center of the white dot was displayed both as pixel coordinates, and by a small red circle centered on the calculated center of the dot. Because the dot had a diameter of 1 *cm*, the relationship between pixel units and *cm* was readily determined, so that the motions of the center of the dot could be expressed in *cm*. This object tracking program was developed using the "IVision LabView Tookit" created by Irene He of Hy-Tek Automation, Waterloo Canada (hytekautomation.com), and Irene He optimized the program for this particular application. The ability of this program to monitor the motions of the Pendulum is excellent. The resolution of the position of the 1 *cm* dot depends on the characteristics of the video camera being used and its distance from the target. We obtained a resolution of about 80 *pixel units*/*cm*, which means that movements of 0.12 *mm* are measureable. The camera used in these experiments was a USB-connected ProScope Model BD-HRB fitted with a 1-10X lens, both obtained from Vernier Software and Technologies (vernier.com). This camera has a tripod mount, so it was readily positioned on a camera tripod (SunPak Model 5800D) and aimed at the Pendulum target. A screenshot of the computer display taken during collection of data points is shown in *Figure 2*. The screenshot shows the data that is displayed continuously include a picture of the 1 *cm* white dot with a red circle located at its calculated center, the dimensions of the dot in *pixel units*, and a graphical display of the motions of the Pendulum during the experiment. The position of the red circle is continually updated, which allows the process of data collection to be monitored throughout the experiment.

The oscillations of the Pendulum were analyzed using the principles of digital signal processing, as described by Lyons [14]. The signal processing program employed was SigView, obtained from SignalLab (sigview.com). It is a very user-friendly program with many features, including Fast Fourier Transform (FFT) signal analysis, BandPass and BandStop filtering, all of which were used in this work.

If the torsional constant (κ) of the nylon monofilament is known, then the amount of force required to rotationally displace the Pendulum by a particular amount from its natural *COO* can be calculated. The equation that relates κ to oscillation of the pendulum is:

Equation 2 $$\omega^2 = \kappa/I$$

where ω is the frequency of oscillation in radians/sec (*cycles/sec * 2* π), κ is the torsional coefficient in *dynes-cm/radian*, and I is the *Moment of Inertia* in *g-cm*^{2}. Whereas the mass of the pendulum is 220 *g*, the *Moment of Inertia* (Mass*r^2) is vague in that the mass is distributed throughout the entire dome of the Pendulum instead of being located at a particular distance *r* from the center. The effective *Moment of Inertia* can be estimated by adding known masses to the rim at the outer edge of the Pendulum, and to graphically-analyze the effects of these masses on the ω of the Pendulum. *Figure 5* shows a plot of ω^2 against $1/I$, the slope of which gives the value of κ. The value of I at each point is $(Mp + Ma)*(17.1\ cm)^2$, where *Mp* is the effective inertial mass of the Pendulum, *Ma* is a mass added to the outer rim of the Pendulum, and 17.1 *cm* is the radius of the Pendulum dome. The value of *Mp* was chosen as that which gives the best fit to the straight line shown in *Figure 5*. The best-fit value for *Mp* was 190 *g*, which means that the entire 220 *g* mass of the Pendulum behaves as if it consisted of a 190 *g* mass concentrated at its outer rim. The slope of this straight line, which is equal to κ, is 2,240 *dyne-cm/radian*, or 39 *dyne-cm* per *deg* of rotation. The physical significance of this is that a force of 39 dynes applied to the end of a 1 *cm* lever-arm produces a torque that can drive a 1 *deg* rotation of the pendulum. Since the pendulum has a radius of 17.1 *cm*, the mean lever-arm is 8.6 *cm*. A force of 4.5 *dynes* applied to this 8.6 *cm* lever-arm can therefore rotate the pendulum by 1 *deg*. Using a conversion factor of 0.00102 *g/dyne*, the force required to drive a rotation of 1 *deg* is that exerted by a 4.6 *mg* mass resting on a horizontal surface at 1 *G*.

References

1 Gutfreund H (1972) Transients and Relaxations, p. 176-228 *In* Gutfreund H (ed.), Enzymes: Physical Principles. John Wiley & Sons, London.

2 Hammes GG, Porter RW, and Stark GR (1971) Relaxation spectra of aspartate transcarbamylase. Interaction of the catalytic subunit with carbamyl phosphate. Biochemistry 10: 1046-1050.

3 Boyer PD (1997) The ATP synthase--a splendid molecular machine. Annual Review of Biochemistry 66: 717-749.

4 Engel GS, Calhoun TR, Read EL, Ahn TK, Mancal T, Cheng YC, Blankenship RE, and Fleming GR (2007) Evidence for wavelike energy transfer through quantum coherence in photosynthetic systems. Nature 446: 782-786.

5 Mohseni M, Rebentrost P, Lloyd S, and Aspuru-Guzik A (2008) Environment-assisted quantum walks in photosynthetic energy transfer. Journal of Chemical Physics 129: 174106.

6 Brookes JC, Hartoutsiou F, Horsfield AP, and Stoneham AM (2007) Could humans recognize odor by phonon tunneling? Physcial Review Letters 98: 038101.

7 Turin L (2002) A method for the calculation of odor character from molecular structure. Journal of Theoretical Biology 216: 367-385.

8 Hameroff S, Nip A, Porter M, and Tuszynski J (2002) Conduction pathways in microtubules, biological quantum computation, and consciousness. Biosystems 64:

149-168.

9 Hameroff SR (2007) The brain is both neurocomputer and quantum computer. Cognitive Science 31: 1035-1045.

10 Hameroff S, Nip A, Porter M, and Tuszynski J (2002) Conduction pathways in microtubules, biological quantum computation, and consciousness. Biosystems 64: 149-168.

11 Hameroff SR (2006) The entwined mysteries of anesthesia and consciousness: is there a common underlying mechanism? Anesthesiology 105: 400-412.

12 Heyes DJ, Sakuma M, de Visser SP, and Scrutton NS (2009) Nuclear quantum tunneling in the light-activated enzyme protochlorophyllide oxidoreductase. Journal of Biological Chemistry 284: 3762-3767.

13 Lloyd S (2008) Enhanced sensitivity of photodetection via quantum illumination. Science 321: 1463-1465.

14 Lyons RG (2004) Understanding digital signal processing. New Jersey: Pearson Education, Inc., Prentice Hall PTR. 665 p.

This manuscript was submitted to PLoS One on June 16, 2009